NASA/TP—2014–218193


# On the Relationship Between Global Land-Ocean Temperature and Various Descriptors of Solar-Geomagnetic Activity and Climate

*Robert M. Wilson*
*Marshall Space Flight Center, Huntsville, Alabama*

***April 2014***

# The NASA STI Program…in Profile

Since its founding, NASA has been dedicated to the advancement of aeronautics and space science. The NASA Scientific and Technical Information (STI) Program Office plays a key part in helping NASA maintain this important role.

The NASA STI Program Office is operated by Langley Research Center, the lead center for NASA's scientific and technical information. The NASA STI Program Office provides access to the NASA STI Database, the largest collection of aeronautical and space science STI in the world. The Program Office is also NASA's institutional mechanism for disseminating the results of its research and development activities. These results are published by NASA in the NASA STI Report Series, which includes the following report types:

- TECHNICAL PUBLICATION. Reports of completed research or a major significant phase of research that present the results of NASA programs and include extensive data or theoretical analysis. Includes compilations of significant scientific and technical data and information deemed to be of continuing reference value. NASA's counterpart of peer-reviewed formal professional papers but has less stringent limitations on manuscript length and extent of graphic presentations.

- TECHNICAL MEMORANDUM. Scientific and technical findings that are preliminary or of specialized interest, e.g., quick release reports, working papers, and bibliographies that contain minimal annotation. Does not contain extensive analysis.

- CONTRACTOR REPORT. Scientific and technical findings by NASA-sponsored contractors and grantees.

- CONFERENCE PUBLICATION. Collected papers from scientific and technical conferences, symposia, seminars, or other meetings sponsored or cosponsored by NASA.

- SPECIAL PUBLICATION. Scientific, technical, or historical information from NASA programs, projects, and mission, often concerned with subjects having substantial public interest.

- TECHNICAL TRANSLATION. English-language translations of foreign scientific and technical material pertinent to NASA's mission.

Specialized services that complement the STI Program Office's diverse offerings include creating custom thesauri, building customized databases, organizing and publishing research results…even providing videos.

For more information about the NASA STI Program Office, see the following:

- Access the NASA STI program home page at <http://www.sti.nasa.gov>

- E-mail your question via the Internet to <help@sti.nasa.gov>

- Phone the NASA STI Help Desk at 757–864–9658

- Write to:
  NASA STI Information Desk
  Mail Stop 148
  NASA Langley Research Center
  Hampton, VA 23681–2199, USA

NASA/TP—2014–218193

# On the Relationship Between Global Land-Ocean Temperature and Various Descriptors of Solar-Geomagnetic Activity and Climate

*Robert M. Wilson*
*Marshall Space Flight Center, Huntsville, Alabama*

National Aeronautics and
Space Administration

Marshall Space Flight Center • Huntsville, Alabama 35812

***April 2014***

Available from:

NASA STI Information Desk
Mail Stop 148
NASA Langley Research Center
Hampton, VA 23681–2199, USA
757–864–9658

This report is also available in electronic form at
<http://www.sti.nasa.gov>

## TABLE OF CONTENTS

## LIST OF FIGURES

## LIST OF FIGURES (Continued)

## LIST OF TABLES

## LIST OF ABBREVIATIONS, ACRONYMS, DESIGNATORS, AND SYMBOLS

| | |
|---|---|
| aa | aa-geomagnetic (index) |
| <aa> | SC-length averaged aa |
| aa(G) | portion of aa index due to G |
| <aa(G)> | SC-length averaged aa(G) |
| aa(I:G) | portion of the aa index remaining following removal of aa(G) |
| <aa(I:G)> | SC-length averaged aa(I:G) |
| aa(I:SSN) | portion of the aa index remaining following removal of aa(SSN) |
| <aa(I:SSN)> | SC-length averaged aa(I:SSN) |
| aamin | minimum amplitude of the aa index |
| aa(SSN) | portion of aa index due to SSN |
| <aa(SSN)> | SC-length averaged aa(SSN) |
| AGGI | annual greenhouse gases index |
| AMO | Atlantic Multidecadal Oscillation (index) |
| <AMO> | SC-length averaged AMO |
| CFC11 | chlorofluorocarbon 11 |
| CFC12 | chlorofluorocarbon 12 |
| $CH_4$ | methane |
| $CO_2$ | carbon dioxide |
| Emax | epoch of maximum amplitude |
| Emin | epoch of minimum amplitude |

| | |
|---|---|
| ENSO | El Niño Southern Oscillation |
| G | number of sunspot groups |
| <G> | SC-length averaged G |
| GLOTI | Global Land-Ocean Temperature Index |
| <GLOTI> | SC-length averaged GLOTI |
| MLCO2 | Mauna Loa $CO_2$ (index) |
| <MLCO2> | SC-length averaged MLCO2 |
| N | number of individual spots |
| NAO | North Atlantic Oscillation (index) |
| <NAO> | SC-length averaged NAO |
| $NO_2$ | nitrous oxide |
| ONI | Oceanic Niño Index |
| PDO | Pacific Decadal Oscillation (index) |
| <PDO> | SC-length averaged PDO |
| Rmax | maximum sunspot amplitude |
| SC | sunspot cycle |
| SOI | Southern Oscillation Index |
| <SOI> | SC-length averaged SOI |
| SSA | sunspot area |
| <SSA> | SC-length averaged SSA |
| SSN | sunspot number |

| | |
|---|---|
| <SSN> | SC-length averaged SSN |
| SST | sea surface temperature |
| THC | thermohaline circulation |
| TP | Technical Publication |

## NOMENCLATURE

| | |
|---|---|
| $a$ | $y$-intercept |
| $b$ | slope |
| $cl$ | confidence level |
| $k$ | reduction coefficient |
| $n$ | number |
| $r$ | coefficient of linear correlation |
| $r^2$ | coefficient of determination |
| $sd$ | standard deviation |
| $se$ | standard error of estimate |
| $t$ | $t$-statistic; elapsed time from Emin |
| $x$ | independent variable |
| $y$ | dependent variable |

TECHNICAL PUBLICATION

# ON THE RELATIONSHIP BETWEEN GLOBAL LAND-OCEAN TEMPERATURE AND VARIOUS DESCRIPTORS OF SOLAR-GEOMAGNETIC ACTIVITY AND CLIMATE

## 1. INTRODUCTION

It has long been recognized that a close association must exist between variations on the Sun and variations in Earth's climate.[1–59] As previously noted by Gray et al.[60] in modern times, it was Sir William Herschel[61] who first speculated (in 1801) that the Sun's variations might directly influence Earth's climate. More recently, Stauning[62] (in 2011) reported that a strong statistical linear correlation appears to exist between averages of solar activity (i.e., sunspot number (SSN)) and global terrestrial temperature anomalies (at least up until 1985) when they are averaged over the same interval lengths (i.e., the sunspot cycle (SC)) but with the global temperature anomaly averages delayed by three years. Examined in this Technical Publication (TP) are determinations of the relative strengths of the inferred statistical correlations (incorporating lag = 0–5 yr) between SC-length averages of the Global Land-Ocean Temperature Index (GLOTI) and SC-length averages of various descriptors of solar-geomagnetic activity and climate, including: (1) SSN, (2) sunspot area (SSA), (3) the number of sunspot groups (G), (4) the aa-geomagnetic (aa) index, (5) aa(SSN) (i.e., that portion of the aa index attributable directly to yearly variations in SSN), (6) the aa(I:SSN) (i.e., that portion of the aa index not attributable to yearly variations in SSN), (7) aa(G) (i.e., that portion of the aa index attributable directly to yearly variations in G), (8) aa(I:G) (i.e., that portion of the aa index not attributable to yearly variations in G), (9) the Atlantic Multidecadal Oscillation (AMO) index, (10) the Southern Oscillation Index (SOI), (11) the North Atlantic Oscillation (NAO) index, (12) the Pacific Decadal Oscillation (PDO) index, and (13) the Mauna Loa carbon dioxide ($CO_2$) (MLCO2) index. Based on the best inferred preferential linear correlation, an estimate is also given for the expected average GLOTI for SC24 (and for SC25), where SC24 is the current ongoing SC, which had a cycle minimum annual amplitude based on SSN, SSA, and G in 2008.

## 2. RESULTS

Figure 1 displays the variation of the annual January–December averages of (a) GLOTI for the yearly interval 1880–2012, and (b) SSN, (c) SSA, and (d) G, where the variations of SSN, SSA, and G span the interval 1875–2012. For GLOTI, it appears to have been trending downwards (cooling) between 1880 and about 1910, but rising (warming) thereafter with a somewhat flattening occurring between about 1935 and 1975. The lowest (coolest) annual value of the GLOTI (to date) measures –0.46 °C in 1909, and the highest (warmest) annual value (to date) measures 0.66 °C in 2010. For the interval 1880–2012, the GLOTI averages 0.013 °C and has a standard deviation $sd = 0.289$ °C. For the interval 1976–2012, which corresponds to SC21 through the rising portion of ongoing SC24, linear regression analysis suggests that the GLOTI is related to year by the expression $y = -33.227 + 0.017x$, having a coefficient of linear correlation $r = 0.896$, a coefficient of determination $r^2 = 0.803$ (meaning that about 80% of the variance in the GLOTI for the interval 1976–2012 can be explained by the inferred regression), a standard error of estimate $se = 0.109$ °C, and a confidence level for the regression $cl > 99.9\%$. Extrapolation of the inferred regression beyond 2012 suggests that the GLOTI possibly will continue to rise with the passage of time at the rate of about 0.017 °C per year, inferring that the GLOTI is expected to measure about $0.80 \pm 0.11$ °C in the year 2020 (the $\pm 1$ *se* prediction interval), unless of course another flattening occurs or another downward trend develops. The annual values of the GLOTI represent deviations (anomalies) from the mean using the base period 1951–1980. (The values of the GLOTI used in this TP were taken from <http://data.giss.nasa.gov/gistemp/tabledata_v3/GLB.Ts+dSST.txt> in October 2013.)

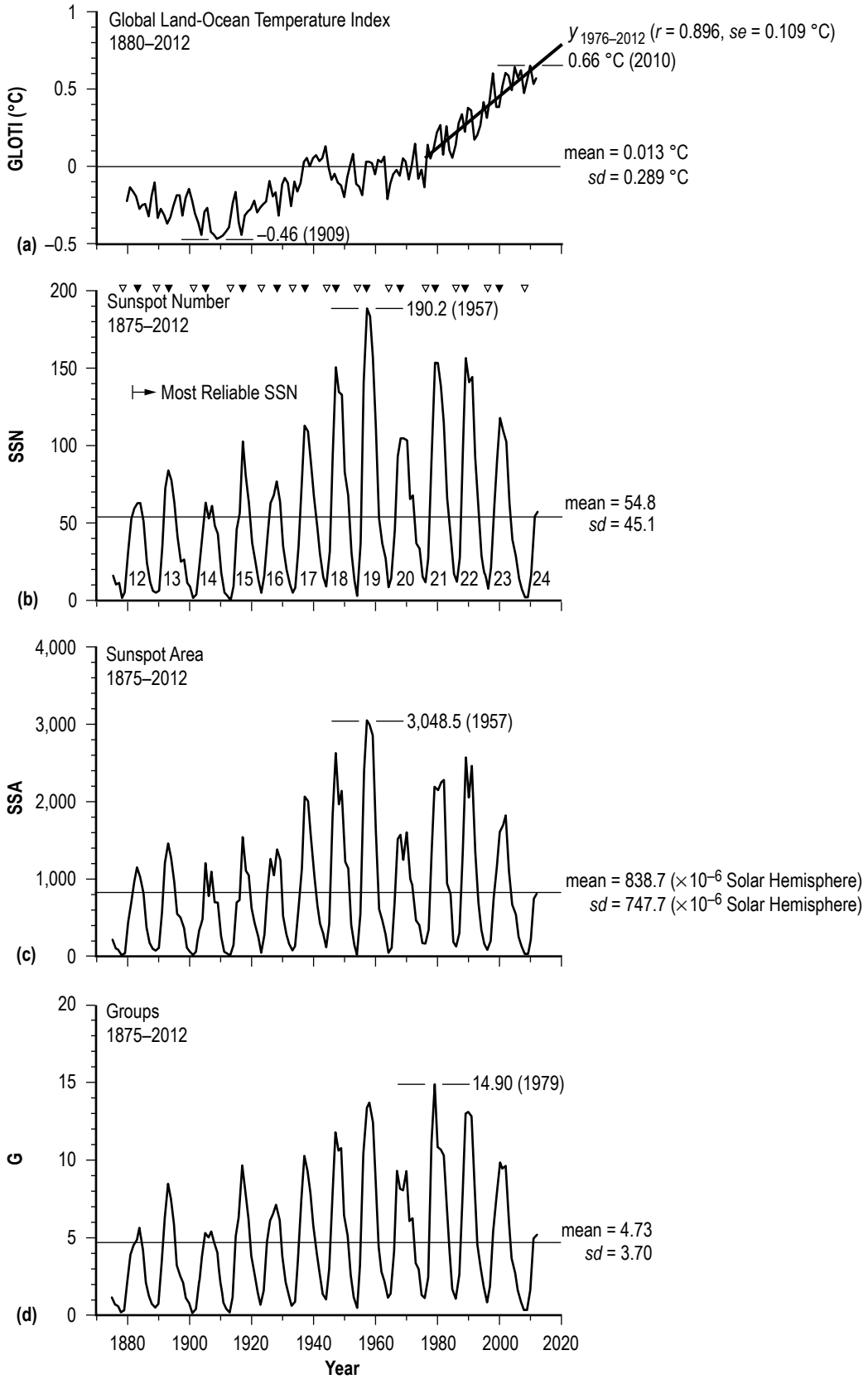


Figure 1. Annual variation of (a) GLOTI, (b) SSN, (c) SSA, and (d) G.

For SSN, its annual variation describes the episodic nature of sunspots, a variation directly attributable to the action of the SC. Plainly, SSN increases from a minimum value marking the onset of the SC (called cycle minimum amplitude and identified by the unfilled triangles) to a maximum value (called cycle maximum amplitude and identified by the filled triangles), which occurs about 3–5 yr after cycle minimum amplitude, and then decreases over time to another minimum amplitude, marking the onset of the next SC. Samuel Heinrich Schwabe[63] was the first to suggest the existence of the 'sunspot cycle,' a term used today to describe the overall variation of SSN over time, where each individual cycle has a minimum-to-minimum length (or period) of about 10–12 yr, with stronger cycles attaining cycle maximum amplitude more quickly than weaker cycles and often also being of shorter duration. In the span of SC12 to SC23, SC19 is the strongest cycle (to date), having the highest cycle maximum amplitude, measuring 190.2 in 1957, while SC14 is the weakest cycle (to date), having cycle maximum amplitude measuring only 63.5, a value slightly smaller than SC12's cycle maximum amplitude of 63.7. For the yearly interval 1875–2012, SSN averages 54.8 and has $sd = 45.1$. While the trend in SSN has been generally upwards between SC14 and SC19, it now appears to be trending downwards. The most reliable values of SSN are those found to span the yearly interval 1882–2012, based on comparison of SSN against group SSN.[64] Prior to 1981, the SSN was determined by the Swiss Federal Observatory based upon observations made at Zürich, Switzerland, and its two branch stations at Arosa and Locarno, and was known as the 'Zürich relative sunspot number.' Beginning in 1981 and continuing through today, the task of determining the SSN, now called the International Sunspot Number, was taken up by the Solar Influences Data Analysis Center, formerly known as the Sunspot Index Data Center, which is located at the Royal Observatory of Belgium <http://www.ngdc.noaa.gov/stp/solar/ssndata.html>. (The SSN values are available online at <http://sidc.oma.be/index.php3>.)

For SSA, its variation generally mimics that of SSN, although the occurrences of some of the extremes sometimes differ. For example, the cycle minimum amplitude for SC20 in terms of SSA is found to precede the cyclic minimum amplitude in terms of SSN by 1 yr, and the cycle maximum amplitude in terms of SSA for SC20, SC21, and SC23 is found to follow the cycle maximum amplitude in terms of SSN by 2, 3, and 2 yr, respectively. Also, about half of the cycles display a more double-peaked appearance in terms of SSA than in terms of SSN. The highest SSA (to date) measures 3,048.5 millionths of a solar hemisphere in 1957, associated with SC19. Interestingly, the cycle maximum amplitude in terms of SSA for SC12 is slightly smaller than that for SC14: 1,148.9 versus 1,195.9 millionths of a solar hemisphere (in contrast to that found using SSN). For the interval 1875–2012, the SSA averages 838.7 millionths of a solar hemisphere and has $sd = 747.7$ millionths of a solar hemisphere. (Annual values of the SSA were taken from <http://solarscience.msfc.nasa.gov/greenwch.shtml>.)

For G, it too generally mimics the behavior of SSN, although like SSA, the individual cycle's maximum amplitude sometimes falls later than is seen in SSN. For example, the cycle maximum amplitude in terms of G for SC12 follows that of the cycle maximum amplitude in terms of SSN by 1 yr. Also, the cycle maximum amplitudes in terms of G for SC14, SC19, and SC22 follow the cycle maximum amplitudes in terms of SSN by 2, 1, and 1 yr, respectively; however, the cycle maximum amplitude in terms of G for SC20 is found to precede the cycle maximum amplitude in terms of SSN by 1 yr (a later-occurring, slightly smaller secondary maximum amplitude in terms of G was observed simultaneously with the maximum amplitude in terms of SSA some 2 yr after the SSN

maximum amplitude). About one-third of the cycles are found to display a double-peaked appearance. The highest G (to date) measures 14.90 in 1979, associated with SC21. For the interval 1875–2012, G averages 4.73 and has $sd = 3.70$. (G is determined directly from the SSA data set.)

Figure 2 depicts the ratios (a) SSN/G, (b) SSA/SSN, and (c) SSA/G for the yearly interval 1875–2012, where the ratios are used to infer the variation of the 'magnetic complexity' of sunspots over individual SCs, with larger ratios, on average, suggesting greater magnetic complexity and smaller ratios suggesting lesser magnetic complexity for each individual SC. For SSN/G, although the maximum value is 19.68 in 1877, the year prior to the minimum amplitude for SC12, this value appears to be erroneous. Recall that the most reliable portion of the SSN record spans 1882 to 2012. A change occurred in the SSN record around 1882, when the $k$ factor was reduced from 1 to 0.6 (Waldmeier[65]) in order to account for smaller spots that were being counted (the relative SSN is calculated based on the formulation $SSN = k(10G + N)$, where $k$ is a reduction coefficient, G is the number of groups, and N is the number of actual individual spots). Because the maximum value of the ratio SSN/G occurs near the minimum amplitude for SC12 (1878), because G is accurately determined from the Royal Greenwich Observatory photographic plate record, and because all SSN/G values during the early yearly interval 1875–1882 (except the value for 1881) are higher than all succeeding values during the interval 1882–2012 together, this suggests that the ratio values SSN/G during the early yearly interval 1875–1881 probably are in error, inferring that the SSN values during the early yearly interval 1875–1881 probably are too high. For the overall yearly interval 1875–2012, SSN/G averages 11.38 and has $sd = 1.84$. Ignoring the early ratios, the largest ratios (to date) measure 14.30 in 1957 (SC19) and 14.28 in 1980 (SC21). Generally, the largest ratio occurs near SC maximum amplitude, and the smallest ratio occurs near SC minimum amplitude for individual cycles. The lowest observed ratio (to date) measures 7.50 in 1911 (late SC14 near cycle minimum amplitude for SC15). For the subyearly interval 1957–2012, one infers that SSN/G appears to be trending downwards, given by the expression $y = 80.572 - 0.035x$, having $r = -0.436$, $r^2 = 0.19$, $se = 1.186$, and $cl > 99.9\%$, inferring that the maximum value of the ratio SSN/G for SC24 probably will be ≤11.56. Interestingly, the observed ratios during the rise of SC24 are smaller than were seen for similar phasing during SC14, suggesting perhaps that SC24 might turn out to be smaller in terms of SSN than that of SC14. (To date, the maximum ratio SSN/G during SC24 measures 11.43, occurring in 2012, having risen from 8.79 in 2009. For an overview of the history of SSN indices, see <http://www.aavso.org/dances-wolfs-short-history-sunspot-indices>.)

For SSA/SSN, because values of SSN appear to be too high for the interval 1875–1882, the early values of SSA/SSN probably are too low. The largest ratio of SSA/SSN (to date) measures 19.77 in 1926 (SC16), slightly larger than two other large ratios, both measuring 19.70 that occurred in 1946 (SC18) and 1982 (SC21). The smallest ratio of SSA/SSN (to date) measures 5.28 in 1964 (SC20, cycle minimum). For the yearly interval 1875–2012, SSA/SSN averages 14.01 and has $sd = 3.20$. Unlike SSN/G, there appears to be no preferential downward trend in SSA/SSN. For the current ongoing SC24, SSA/SSN has varied between 7.86 in 2008 and 13.86 in 2012, values that are lower than were seen in SC14, which varied between 10.33 and 18.83 for similar phasing (1901–1905).

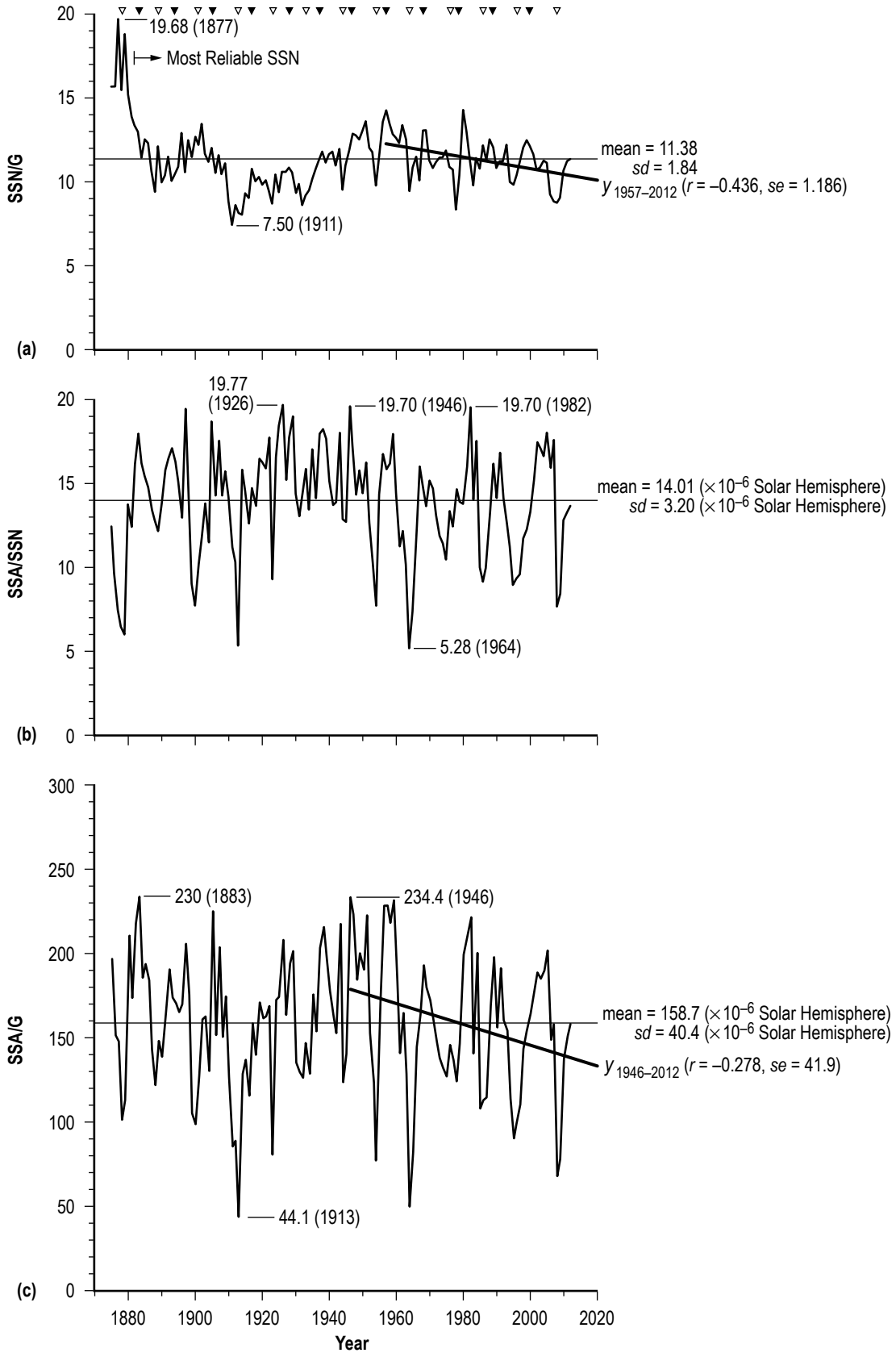


Figure 2. Annual variation of ratios (a) SSN/G, (b) SSA/SSN, and (c) SSA/G.

For SSA/G, the two largest ratios (to date) measure 230 in 1883 (SC12) and 234.4 in 1946 (SC18). The smallest ratio (to date) measures 44.1 in 1913 (SC15, cycle minimum). For the yearly interval 1875–2012, SSA/G averages 158.7 and has $sd = 40.4$. Like the ratio SSN/G, the ratio SSA/G appears to be trending downwards with the passage of time, given by the expression $y = 1{,}379.3 - 0.617x$, having $r = -0.278$, $r^2 = 0.08$, $se = 41.9$, and $cl > 95\%$. For the current ongoing SC24, SSA/G has varied between 69.1 in 2008 and 157.8 in 2012, values that are lower than were seen in SC14, which varied between 126.8 and 225.2 for similar phasing (1901–1905).

Figure 3 displays the annual values of (a) the aa index, (b) aa(SSN), and (c) aa(G) for the yearly interval 1875–2012. For the aa index, it has varied between 6.1 nT in 1901 (SC14) and 37.1 nT in 2003 (SC23), averaging 19.3 nT and having $sd = 6.3$ nT for the overall yearly interval 1875–2012. The aa index correlates strongly with the solar wind speed and the occurrences of the southward-pointing interplanetary magnetic field at Earth.[66–68] It should be noted that Svalgaard et al.[69] have suggested that the observed aa index values before 1957 be increased by about 3 nT to compensate for movements of the magnetometers in Australia, which are used in the computation of the aa index. Doing so, one finds that the minimum amplitude of the aa index value (aamin) would now become 8.6 nT, which is the minimum amplitude value for SC24 in 2009. (The value of aamin usually follows SSN cycle minimum by one year and correlates strongly with the later-occurring SSN cycle maximum for each individual SC.)[66,70–72]

For aa(SSN) and aa(G), as previously noted, these parameters represent those portions of the aa index value directly attributable to the variation of the SC (dependent upon whether one uses SSN or G, respectively, to describe the SC). For aa(SSN), its peak value (to date) measures 26.2 nT in 1957 (SC19), and aa(SSN) is found to average 11.6 nT and have $sd = 4.8$ nT for the yearly interval 1875–2012, while for aa(G), its peak value (to date) measures 22.5 nT in 1979 (SC21), and aa(G) is found to average 11.1 nT and have $sd = 4.1$ nT. (Notice that the minimum value for aa(G) is of comparable size for SC12, SC14, SC15, and SC24.)

Figure 4 displays scatter plots of aa versus (a) SSN and (b) G, where the diagonal lines represent aa(SSN) and aa(G), respectively, following the approach used by Feyman (ignoring the lone outlier associated with SSN for 1980, the point plotted below the aa(SSN) line).[73,74] In the scatter plots, $aa(SSN) = 5.81 + 0.107SSN$, and $aa(G) = 5.85 + 1.117G$. As an example, SC19 had a maximum amplitude in terms of SSN (Rmax) equal to 190.2 in 1957, thus yielding aa(SSN) = 26.2 nT.

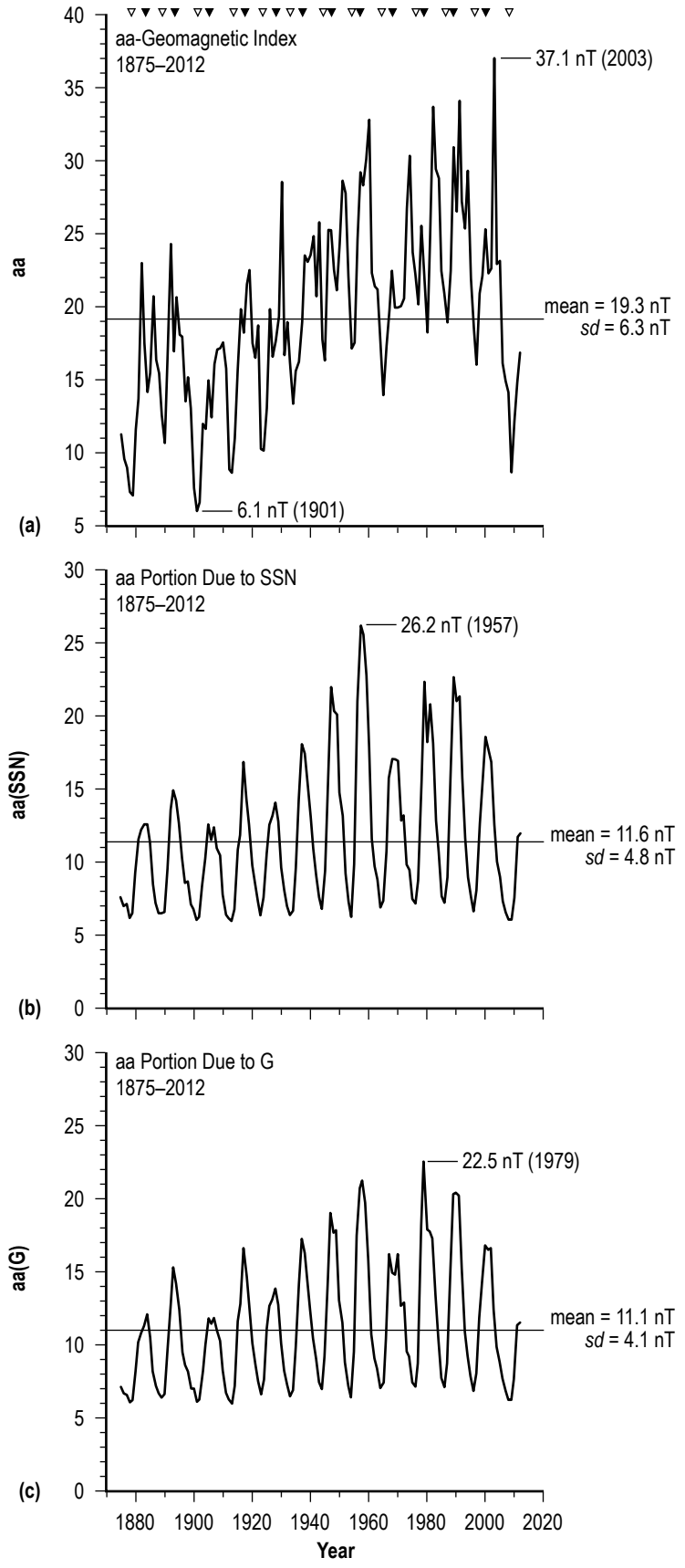


Figure 3. Annual variation of (a) the aa index, (b) aa(SSN), and (c) aa(G).

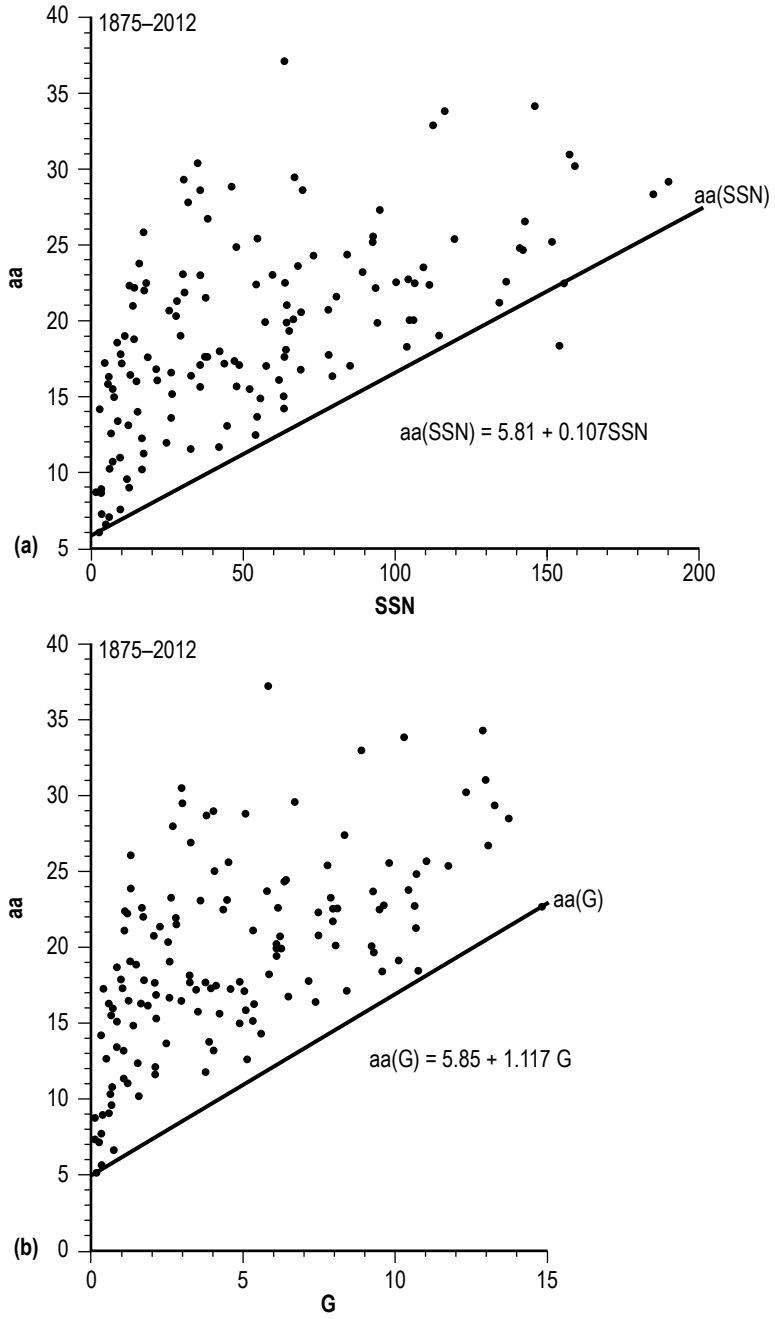


Figure 4. Scatter plots of (a) aa versus SSN and (b) aa versus G.

Figure 5 shows the annual values of (a) aa(I:SSN) and (b) aa(I:G), those portions of the aa index not attributed to SSN or G, respectively. Recall that Feyman suggested that the aa index can be simply decomposed into two components: aa(SSN) and aa(I:SSN) (or aa(G) and aa(I:G)).[73,74] The aa(SSN) (or aa(G)) component is that component due to the sporadic, short-lived events occurring on the Sun, which varies over the SC in phase with SSN (or G). The aa(I:SSN) (or aa(I:G)) component is that component due to the recurrent, long-lived events, like coronal holes (regions on the Sun that are the sources of the high-speed recurrent streams of solar wind, typically seen

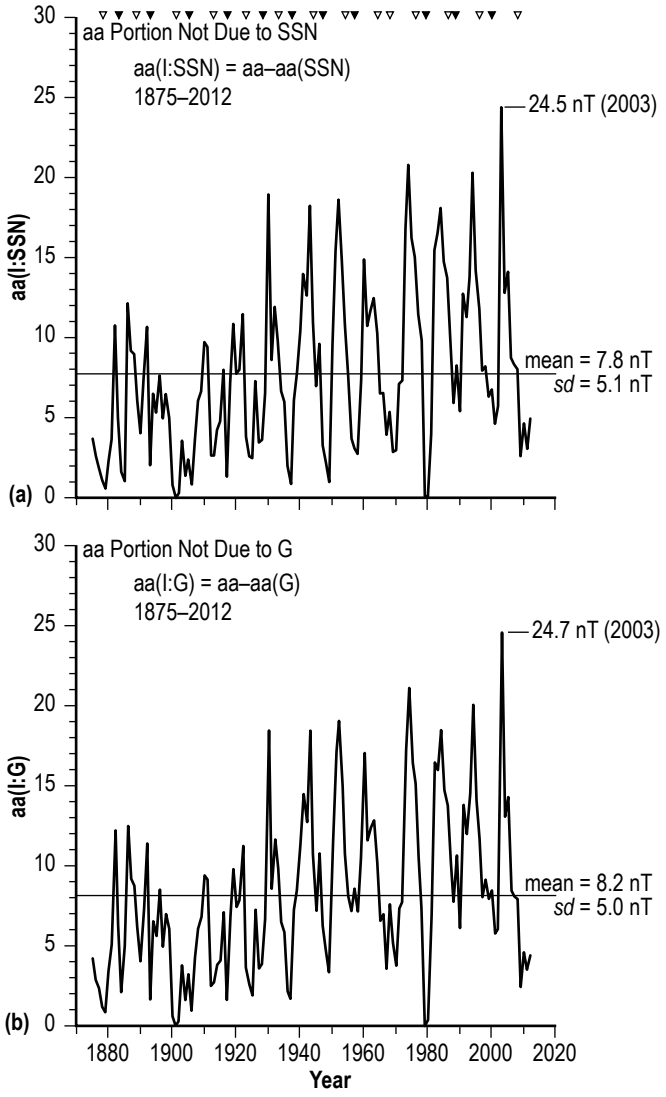


Figure 5. Annual variation of (a) aa(I:SSN) and (b) aa(I:G).

during the declining portion of the SC between SSN cycle maximum amplitude and the succeeding cycle minimum amplitude marking the onset of the next SC) occurring on the Sun, which varies over the SC but is out of phase with respect to the phasing of aa(SSN) (or aa(G)). For aa(I:SSN), its peak value (to date) measures 24.5 nT in 2003, and for the yearly interval 1875–2012, aa(I:SSN) averages 7.8 nT and has $sd = 5.1$ nT. For aa(I:G), its peak value (to date) measures 24.7 nT in 2003, and for the yearly interval 1875–2012, aa(I:G) averages 8.2 nT and has $sd = 5.0$ nT. (In the above example for SC19, the maximum amplitude of aa(I:SSN) is found to be 15 nT in 1960.)

Figure 6 displays the variation of the asymmetry in the aa index for (a) [aa(I:SSN) – aa(SSN)]/aa and (b) [aa(I:G) – aa(G)]/aa for the yearly interval 1875–2012. When the values are negative, this simply means that the sporadic component contributes more to the value of the aa index than the recurrent component, the opposite being true for positive values. For [aa(I:SSN) – aa(SSN)]/aa, it averages –0.24 and has $sd = 0.37$. For [aa(I:G) – aa(G)]/aa, it averages –0.20 and has $sd = 0.35$. Thus,

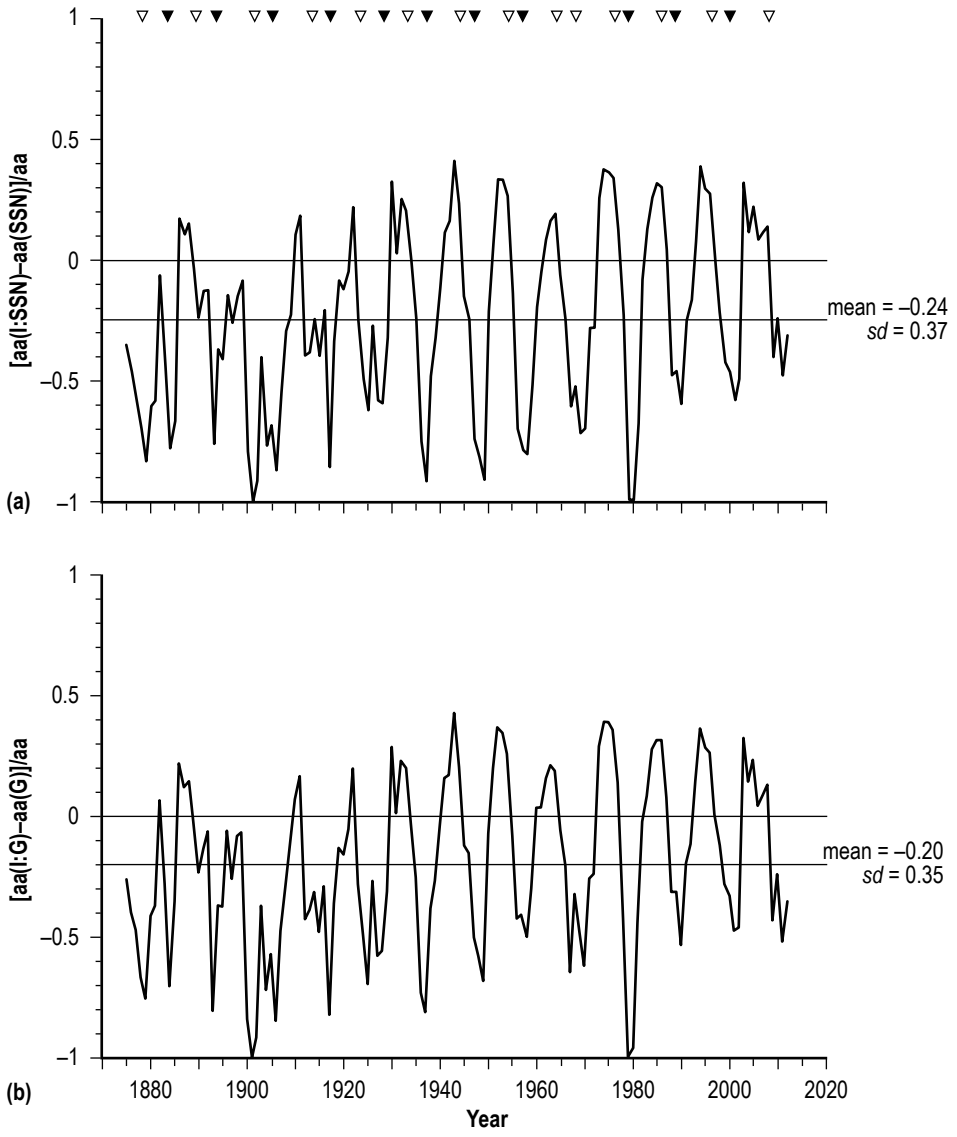


Figure 6. Annual variation of asymmetries (a) [aa(I:SSN) – aa(SSN)]/aa and (b) [aa(I:G) – aa(G)]/aa.

on average, the sporadic component has been the stronger contributor to the value of the aa index than the recurrent component. Close inspection reveals that this was especially true during SC14 (1901–1912).

Table 1a identifies the epochs of the cycle minimum (Emin) and maximum (Emax), the minimum-to-minimum SC-length, the Rmax, the aamin, and SC averages of SSN, SSA, G, aa, aa(SSN), aa(I:SSN), aa(G), and aa(I:G) for each SC12–SC23. Also, table 1b identifies SC averages for the GLOTI, incorporating lags of 0–5 yr, relative to Emin.

Table 1a. Sunspot cycle epochs and selected parametric values—epochs and values.

| Cycle | Emin | Emax | Length | Rmax | aamin | <SSN> | <SSA> | <G> | <aa> | <aa(SSN)> | <aa(I:SSN)> | <aa(G)> | <aa(I:G)> |
|---|---|---|---|---|---|---|---|---|---|---|---|---|---|
| 12 | 1878 | 1883 | 11 | 63.7 | 7.1 | 34.6 | 526.4 | 2.70 | 14.8 | 9.5 | 5.1 | 8.9 | 6.1 |
| 13 | 1889 | 1893 | 12 | 85.1 | 10.7 | 38.8 | 607.2 | 3.54 | 15.7 | 10.0 | 5.7 | 9.8 | 5.9 |
| 14 | 1901 | 1905 | 12 | 63.5 | 6.1 | 31.1 | 477.8 | 2.84 | 13.1 | 9.1 | 3.9 | 9.0 | 4.0 |
| 15 | 1913 | 1917 | 10 | 103.9 | 8.7 | 44.2 | 657.3 | 4.44 | 17.1 | 10.5 | 6.7 | 10.8 | 6.3 |
| 16 | 1923 | 1928 | 10 | 77.8 | 10.2 | 41.0 | 706.9 | 4.00 | 17.2 | 10.2 | 7.0 | 10.3 | 6.9 |
| 17 | 1933 | 1937 | 11 | 114.4 | 13.4 | 55.0 | 914.2 | 4.64 | 20.3 | 11.7 | 8.6 | 11.3 | 9.0 |
| 18 | 1944 | 1944 | 10 | 151.6 | 16.4 | 75.7 | 1,203.4 | 6.02 | 23.2 | 13.9 | 9.3 | 12.6 | 10.6 |
| 19 | 1954 | 1957 | 10 | 190.2 | 17.2 | 95.0 | 1,492.0 | 7.18 | 24.6 | 16.0 | 8.6 | 13.9 | 10.7 |
| 20 | 1964 | 1968 | 12 | 105.9 | 14.0 | 58.8 | 819.2 | 5.09 | 21.1 | 12.1 | 9.0 | 11.5 | 9.5 |
| 21 | 1976 | 1979 | 10 | 155.4 | 20.3* | 82.9 | 1,273.0 | 7.39 | 24.9 | 13.8 | 11.8 | 14.1 | 10.8 |
| 22 | 1986 | 1989 | 10 | 157.6 | 19.0 | 78.5 | 1,141.7 | 6.82 | 25.9 | 14.2 | 11.6 | 13.5 | 12.4 |
| 23 | 1996 | 2000 | 12 | 119.6 | 16.1 | 56.6 | 839.0 | 4.92 | 21.9 | 11.9 | 10.1 | 11.4 | 10.6 |
| 24 | 2008 | 2012? | – | 57.5? | 8.7 | – | – | – | – | – | – | – | – |

Note: * SC21 had an aamin in the vicinity of Emin; however, its observed aamin was 18.3 occurring near Emax.

Table 1b. Sunspot cycle epochs and selected parametric values—SC-length GLOTI values for lag = 0–5 yr.

| | Lag (yr) | | | | | |
|---|---|---|---|---|---|---|
| Cycle | 0 | 1 | 2 | 3 | 4 | 5 |
| 12 | – | – | –0.217 | –0.222 | –0.238 | –0.256 |
| 13 | –0.246 | –0.241 | –0.253 | –0.260 | –0.271 | –0.265 |
| 14 | –0.373 | –0.388 | –0.382 | –0.365 | –0.358 | –0.371 |
| 15 | –0.295 | –0.282 | –0.283 | –0.289 | –0.262 | –0.236 |
| 16 | –0.174 | –0.173 | –0.158 | –0.151 | –0.152 | –0.131 |
| 17 | –0.022 | 0.014 | 0.023 | 0.029 | 0.023 | 0.023 |
| 18 | –0.032 | –0.057 | –0.070 | –0.080 | –0.072 | –0.059 |
| 19 | –0.018 | –0.027 | –0.025 | –0.011 | –0.016 | –0.025 |
| 20 | –0.023 | –0.016 | 0.005 | 0.013 | 0.024 | 0.048 |
| 21 | 0.128 | 0.155 | 0.169 | 0.198 | 0.210 | 0.226 |
| 22 | 0.291 | 0.309 | 0.325 | 0.351 | 0.367 | 0.368 |
| 23 | 0.526 | 0.539 | 0.551 | 0.555 | 0.568 | 0.583 |

Figure 7 plots the SC averages of the GLOTI (taken from table 1b). For all lags (0–5 yr), it is quite apparent that SC averages of GLOTI track upwards with the passage of time, with a noticeable flattening spanning SC17–SC20. Since SC20 (1964–1975), the GLOTI values have consistently risen with the passage of time, with the current ongoing rise in the SC average value of the GLOTI being of steeper slope than the previous one found for the preceding interval SC14–SC17.

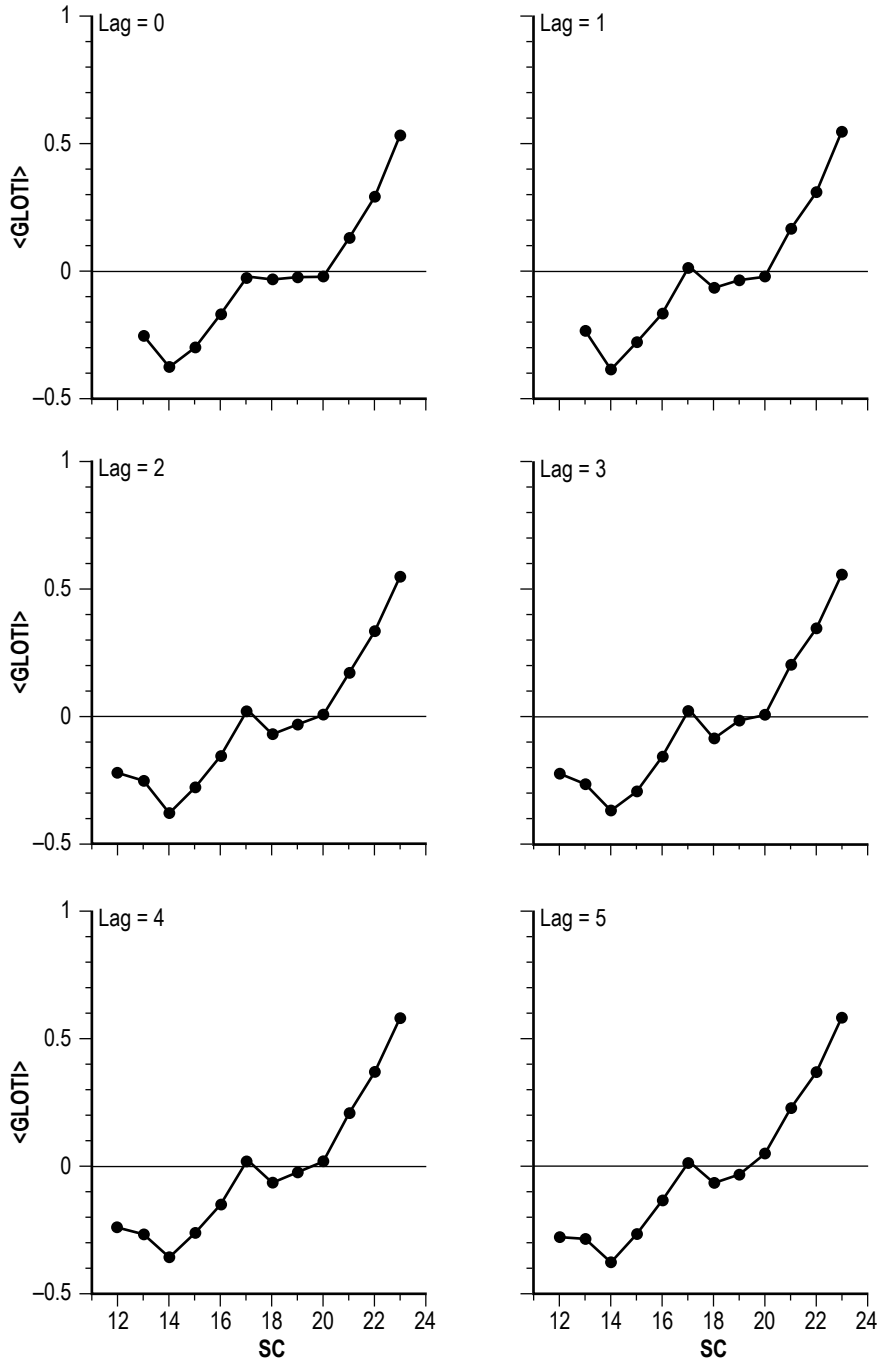


Figure 7. Variation of SC averages of <GLOTI> for lag 0–5 yr.

Figure 8 plots the SC averages of the eight solar-geomagnetic parameters (taken from table 1a). Some similarity is noticeable between these parameters and <GLOTI>, in particular with <aa(I:SSN)> and <aa(I:G)>.

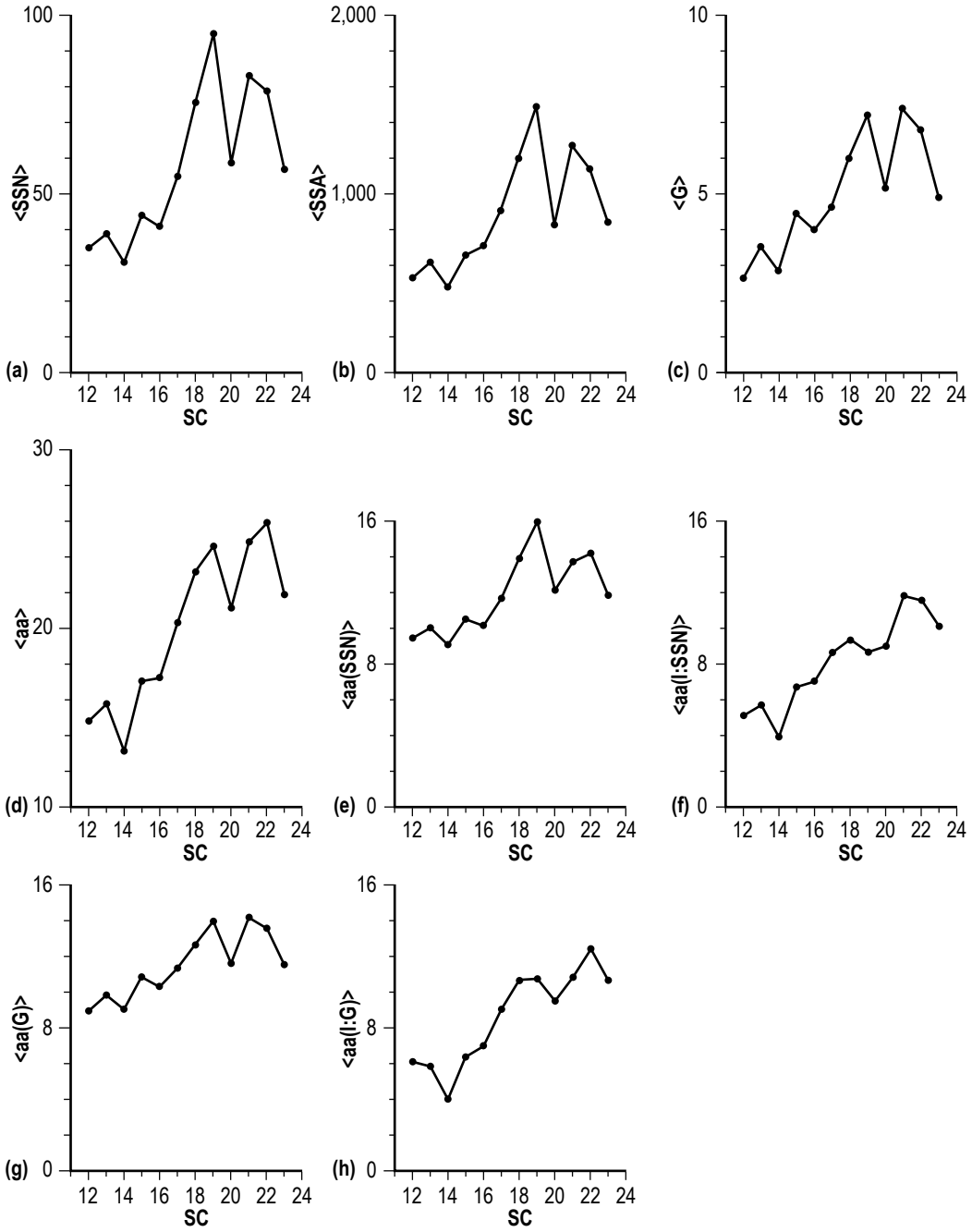


Figure 8. Variation of SC averages of (a) <SSN>, (b) <SSA>, (c) <G>, (d) <aa>, (e) <aa(SSN)>, (f) <aa(I:SSN)>, (g) <aa(G)>, and (h) <aa(I:G)>.

Figure 9a displays the scatter plots of <GLOTI> versus <SSN>, and figure 9b displays scatter plots of <GLOTI> versus <aa> for lags of 0–5 yr for the groupings SC12–SC21 and SC12–SC23. It is apparent that SC23 (and possibly SC22, both plotted as filled squares) is a statistical outlier with respect to the inferred regression based on SC12–SC21. In contrast to that of Stauning,[62] the strongest inferred linear correlation between <GLOTI> and <SSN> using SC12–SC21 is the one incorporating lag = 0 yr, having $r = 0.83$ and $se = 0.09$ °C. (This is also true for <GLOTI> versus <aa> for lag = 0 yr, having $r = 0.93$ and $se = 0.07$ °C.)

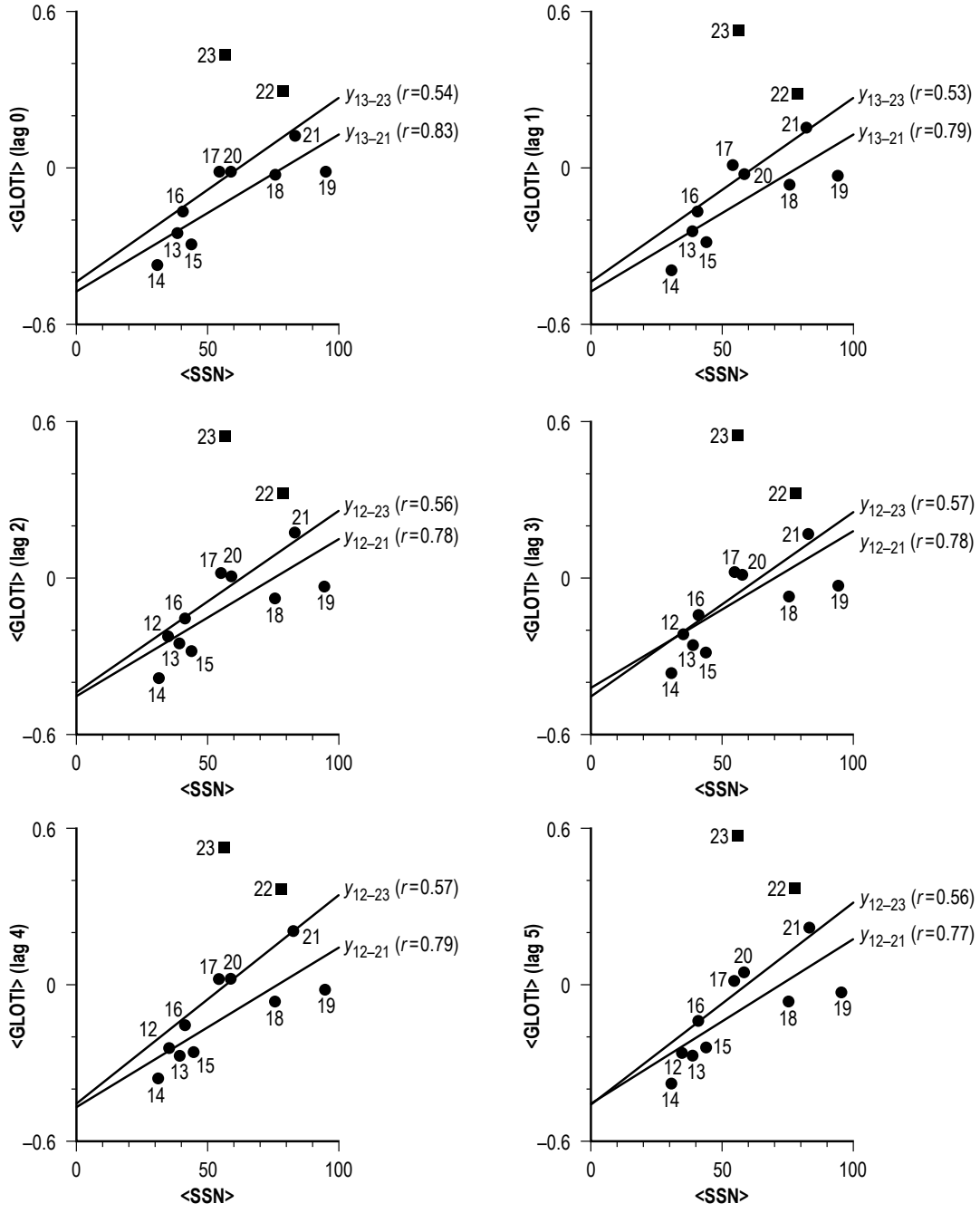


Figure 9a. Scatter plots of <GLOTI> versus <SSN> for lag 0–5 yr.

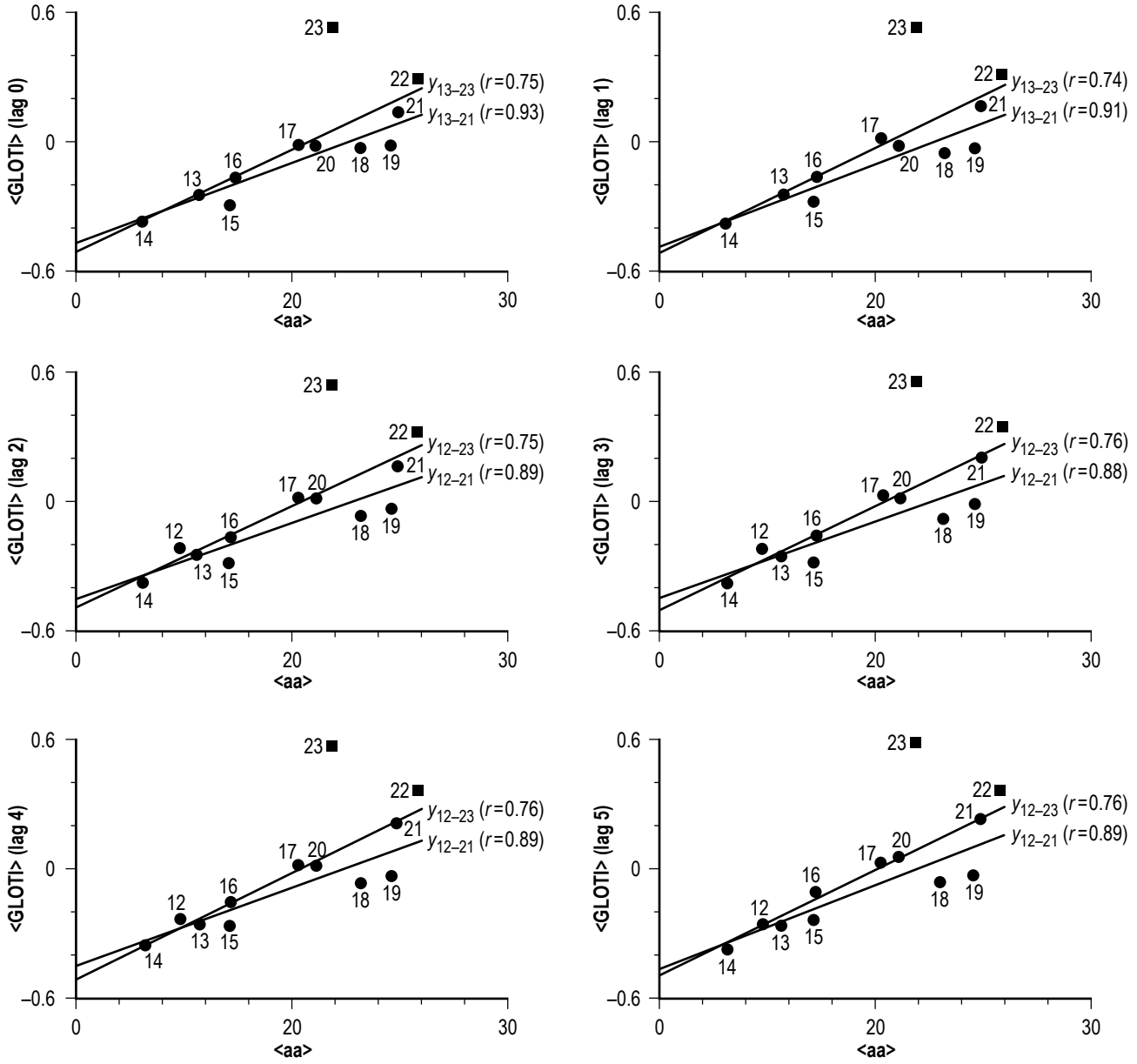


Figure 9b. Scatter plots of <GLOTI> versus <aa> for lag 0–5 yr.

Figure 10a shows the scatter plots of <GLOTI> versus <aa(I:SSN)>, and figure 10b shows the scatter plots of <GLOTI> versus <aa(I:G)> for lags of 0–5 yr. All inferred correlations are stronger than those based on either <SSN> or <aa> (shown in figs. 9a and 9b). The strongest inferred linear correlation using the grouping SC12–SC21 appears to be that of <GLOTI> versus <aa(I:SSN)> for lag = 5 yr, having $r = 0.97$ and $se = 0.05$ °C. (For <GLOTI> versus <aa(I:G)>, the strongest inferred correlation using the grouping SC12–SC21 appears to be the one incorporating lag = 0 yr, having $r = 0.95$ and $se = 0.05$ °C.)

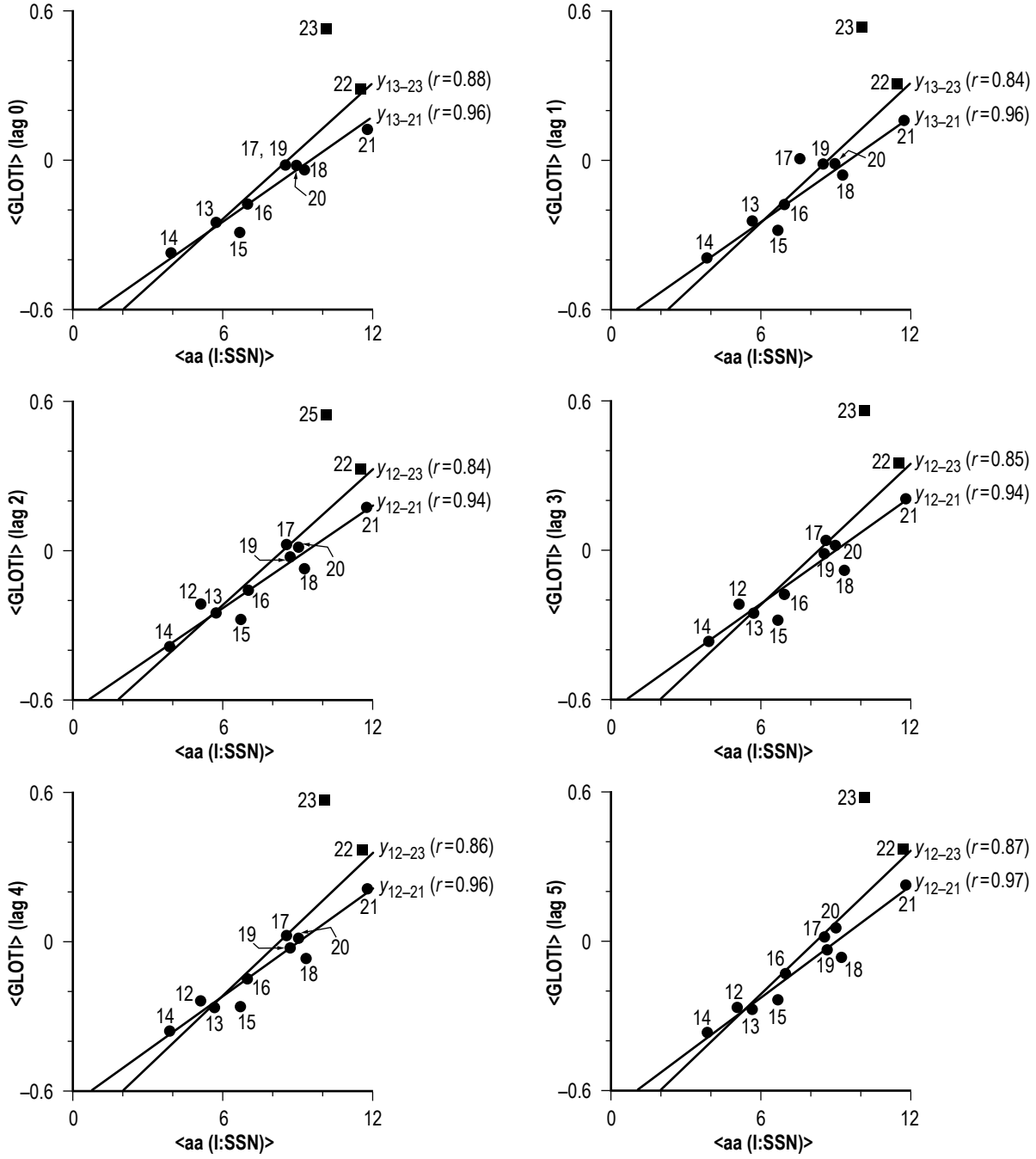


Figure 10a. Scatter plots of <GLOTI> versus <aa(I:SSN)> for lag 0–5 yr.

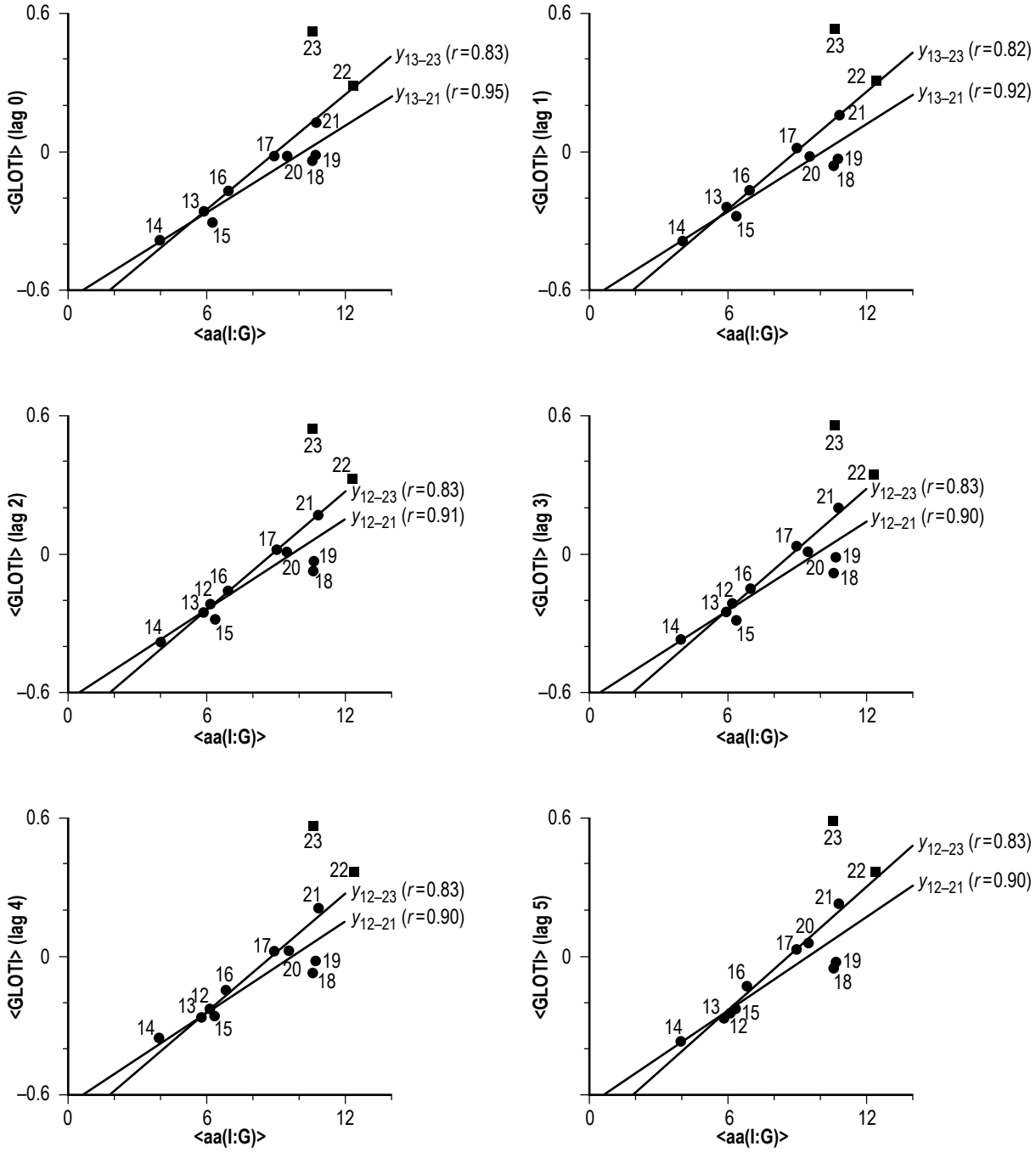


Figure 10b. Scatter plots of <GLOTI> versus <aa(I:G)> for lag 0–5 yr.

Table 2 provides the statistics for each of the correlations of <GLOTI> versus the eight solar-geomagnetic parameters, arranged according to $r^2$, the coefficient of determination, for both groupings SC12–SC21 and SC12–SC23 and for lags 0–5 yr. For every case, the strongest inferred linear correlation is the one based on <aa(I:SSN)>. In table 2, the statistic *a* is the *y*-intercept, *b* is the slope, *r* is the coefficient of linear correlation, $r^2$ is the coefficient of determination, *se* is the standard error of estimate, *t* is the *t*-statistic for determining the statistical importance of the inferred linear correlation, *n* is the number of SC used in the analysis, and *cl* is the confidence level of the inferred linear correlation (based on *n* and *t*).

Table 2. Correlations of SC averages of GLOTI against SC averages of selected parameters of solar-geomagnetic activity, incorporating lag 0–5 yr.

| Lag 0, SC13–SC21 | | | | | | | | |
|---|---|---|---|---|---|---|---|---|
| Parameter | *a* | *b* | *r* | $r^2$ | *se* | *t* | *n* | *cl* |
| <aa(I:SSN)> | –0.651 | 0.068 | 0.962 | 0.926 | 0.047 | 9.449 | 9 | >99.9% |
| <aa(I:G)> | –0.627 | 0.062 | 0.950 | 0.902 | 0.053 | 8.262 | 9 | >99.9% |
| <aa> | –0.838 | 0.037 | 0.934 | 0.873 | 0.069 | 6.327 | 9 | >99.9% |
| <aa(G)> | –1.042 | 0.081 | 0.872 | 0.761 | 0.089 | 4.550 | 9 | >99.5% |
| <G> | –0.564 | 0.089 | 0.860 | 0.740 | 0.089 | 4.465 | 9 | >99.5% |
| <SSN> | –0.474 | 0.006 | 0.831 | 0.691 | 0.093 | 4.038 | 9 | >99.5% |
| <SSA> | –0.470 | 0.0004 | 0.824 | 0.679 | 0.103 | 3.784 | 9 | >99% |
| <aa(SSN)> | –0.804 | 0.058 | 0.799 | 0.638 | 0.107 | 3.449 | 9 | >98% |

| Lag 0, SC13–SC23 | | | | | | | | |
|---|---|---|---|---|---|---|---|---|
| Parameter | *a* | *b* | *r* | $r^2$ | *se* | *t* | *n* | *cl* |
| <aa(I:SSN)> | –0.783 | 0.091 | 0.834 | 0.695 | 0.153 | 4.544 | 11 | >99.8% |
| <aa(I:G)> | –0.750 | 0.083 | 0.827 | 0.684 | 0.156 | 4.422 | 11 | >99.8% |
| <aa> | –0.980 | 0.047 | 0.746 | 0.556 | 0.185 | 3.370 | 11 | >99.5% |
| <aa(G)> | –1.078 | 0.091 | 0.583 | 0.339 | 0.225 | 2.159 | 11 | >90% |
| <G> | –0.538 | 0.100 | 0.573 | 0.328 | 0.227 | 2.099 | 11 | >90% |
| <SSN> | –0.434 | 0.007 | 0.542 | 0.293 | 0.233 | 1.966 | 11 | >90% |
| <aa(SSN)> | –0.834 | 0.067 | 0.543 | 0.295 | 0.233 | 1.942 | 11 | >90% |
| <SSA> | –0.394 | 0.0004 | 0.488 | 0.238 | 0.242 | 1.656 | 11 | <90% |

| Lag 1, SC13–SC21 | | | | | | | | |
|---|---|---|---|---|---|---|---|---|
| Parameter | *a* | *b* | *r* | $r^2$ | *se* | *t* | *n* | *cl* |
| <aa(I:SSN)> | –0.671 | 0.071 | 0.962 | 0.925 | 0.049 | 9.523 | 9 | >99.9% |
| <aa(I:G)> | –0.631 | 0.063 | 0.923 | 0.852 | 0.069 | 6.445 | 9 | >99.9% |
| <aa> | –0.845 | 0.037 | 0.908 | 0.824 | 0.074 | 5.894 | 9 | >99.9% |
| <aa(G)> | –1.053 | 0.082 | 0.848 | 0.718 | 0.097 | 4.203 | 9 | >99.5% |
| <G> | –0.566 | 0.090 | 0.833 | 0.694 | 0.100 | 4.009 | 9 | >99% |
| <SSN> | –0.468 | 0.006 | 0.791 | 0.626 | 0.109 | 3.443 | 9 | >99% |
| <SSA> | –0.464 | 0.0004 | 0.785 | 0.616 | 0.117 | 3.327 | 9 | >98% |
| <aa(SSN)> | –0.791 | 0.057 | 0.754 | 0.568 | 0.120 | 3.028 | 9 | >98% |

| Lag 1, SC13–SC23 | | | | | | | | |
|---|---|---|---|---|---|---|---|---|
| Parameter | *a* | *b* | *r* | $r^2$ | *se* | *t* | *n* | *cl* |
| <aa(I:SSN)> | –0.804 | 0.094 | 0.841 | 0.707 | 0.154 | 4.652 | 11 | >99.8% |
| <aa(I:G)> | –0.758 | 0.085 | 0.821 | 0.674 | 0.162 | 4.359 | 11 | >99.8% |
| <aa> | –0.993 | 0.048 | 0.741 | 0.549 | 0.191 | 3.326 | 11 | >99% |
| <aa(G)> | –1.094 | 0.093 | 0.580 | 0.336 | 0.232 | 2.143 | 11 | >90% |
| <G> | –0.541 | 0.102 | 0.568 | 0.323 | 0.234 | 2.076 | 11 | >90% |
| <SSN> | –0.429 | 0.007 | 0.530 | 0.280 | 0.241 | 1.896 | 11 | >90% |
| <aa(SSN)> | –0.827 | 0.067 | 0.528 | 0.279 | 0.242 | 1.870 | 11 | >90% |
| <SSA> | –0.388 | 0.0004 | 0.476 | 0.226 | 0.251 | 1.600 | 11 | <90% |

| Lag 2, SC12–SC21 | | | | | | | | |
|---|---|---|---|---|---|---|---|---|
| Parameter | *a* | *b* | *r* | $r^2$ | *se* | *t* | *n* | *cl* |
| <aa(I:SSN)> | –0.634 | 0.068 | 0.945 | 0.893 | 0.058 | 8.186 | 10 | >99.9% |
| <aa(I:G)> | –0.622 | 0.063 | 0.911 | 0.830 | 0.073 | 6.257 | 10 | >99.9% |
| <aa> | –0.800 | 0.035 | 0.888 | 0.788 | 0.076 | 5.831 | 10 | >99.9% |
| <aa(G)> | –0.957 | 0.075 | 0.821 | 0.674 | 0.104 | 4.003 | 10 | >99.5% |
| <G> | –0.513 | 0.082 | 0.808 | 0.653 | 0.104 | 3.897 | 10 | >99.5% |
| <SSN> | –0.451 | 0.006 | 0.780 | 0.608 | 0.113 | 3.527 | 10 | >99% |
| <SSA> | –0.444 | 0.0004 | 0.771 | 0.595 | 0.122 | 3.395 | 10 | >99% |
| <aa(SSN)> | –0.765 | 0.055 | 0.744 | 0.553 | 0.118 | 3.176 | 10 | >98% |

| Lag 2, SC13–SC23 | | | | | | | | |
|---|---|---|---|---|---|---|---|---|
| Parameter | *a* | *b* | *r* | $r^2$ | *se* | *t* | *n* | *cl* |
| <aa(I:SSN)> | –0.766 | 0.091 | 0.843 | 0.711 | 0.152 | 4.946 | 12 | >99.9% |
| <aa(I:G)> | –0.755 | 0.085 | 0.827 | 0.685 | 0.159 | 4.657 | 12 | >99.9% |
| <aa> | –0.962 | 0.047 | 0.750 | 0.562 | 0.187 | 3.599 | 12 | >99.5% |
| <aa(G)> | –1.057 | 0.090 | 0.602 | 0.363 | 0.225 | 2.380 | 12 | >95% |
| <G> | –0.520 | 0.099 | 0.592 | 0.351 | 0.228 | 2.316 | 12 | >95% |
| <SSN> | –0.844 | 0.069 | 0.554 | 0.307 | 0.235 | 2.112 | 12 | >90% |
| <aa(SSN)> | –0.437 | 0.007 | 0.556 | 0.309 | 0.235 | 2.073 | 12 | >90% |
| <SSA> | –0.400 | 0.0004 | 0.505 | 0.255 | 0.245 | 1.753 | 12 | <90% |

Table 2. Correlations of SC averages of GLOTI against SC averages of selected parameters of solar-geomagnetic activity, incorporating lag 0–5 yr (Continued).

| Lag 3, SC12–SC21 | | | | | | | | |
|---|---|---|---|---|---|---|---|---|
| Parameter | *a* | *b* | *r* | $r^2$ | *se* | *t* | *n* | *cl* |
| <aa(I:SSN)> | –0.644 | 0.070 | 0.940 | 0.883 | 0.063 | 7.767 | 10 | >99.9% |
| <aa(I:G)> | –0.627 | 0.064 | 0.898 | 0.806 | 0.080 | 5.823 | 10 | >99.9% |
| <aa> | –0.814 | 0.036 | 0.882 | 0.777 | 0.082 | 5.557 | 10 | >99.9% |
| <aa(G)> | –0.984 | 0.078 | 0.833 | 0.678 | 0.108 | 4.020 | 10 | >99.5% |
| <G> | –0.523 | 0.086 | 0.811 | 0.658 | 0.109 | 3.907 | 10 | >99.5% |
| <SSN> | –0.457 | 0.006 | 0.780 | 0.608 | 0.113 | 3.523 | 10 | >99% |
| <SSA> | –0.451 | 0.0004 | 0.770 | 0.593 | 0.121 | 3.424 | 10 | >99% |
| <aa(SSN)> | –0.780 | 0.057 | 0.740 | 0.548 | 0.124 | 3.115 | 10 | >98% |

| Lag 3, SC12–SC23 | | | | | | | | |
|---|---|---|---|---|---|---|---|---|
| Parameter | *a* | *b* | *r* | $r^2$ | *se* | *t* | *n* | *cl* |
| <aa(I:SSN)> | –0.780 | 0.094 | 0.849 | 0.722 | 0.111 | 6.973 | 12 | >99.9% |
| <aa(I:G)> | –0.764 | 0.087 | 0.830 | 0.689 | 0.161 | 4.702 | 12 | >99.9% |
| <aa> | –0.983 | 0.048 | 0.757 | 0.573 | 0.192 | 3.579 | 12 | >99% |
| <aa(G)> | –1.093 | 0.094 | 0.615 | 0.378 | 0.227 | 2.467 | 12 | >95% |
| <G> | –0.534 | 0.104 | 0.605 | 0.366 | 0.229 | 2.417 | 12 | >95% |
| <SSN> | –0.866 | 0.071 | 0.562 | 0.316 | 0.238 | 2.145 | 12 | >90% |
| <aa(SSN)> | –0.447 | 0.007 | 0.566 | 0.321 | 0.239 | 2.037 | 12 | >90% |
| <SSA> | –0.408 | 0.0004 | 0.515 | 0.266 | 0.249 | 1.720 | 12 | <90% |

| Lag 4, SC12–SC21 | | | | | | | | |
|---|---|---|---|---|---|---|---|---|
| Parameter | *a* | *b* | *r* | $r^2$ | *se* | *t* | *n* | *cl* |
| <aa(I:SSN)> | –0.654 | 0.072 | 0.956 | 0.913 | 0.056 | 8.956 | 10 | >99.9% |
| <aa(I:G)> | –0.630 | 0.065 | 0.901 | 0.812 | 0.081 | 5.886 | 10 | >99.9% |
| <aa> | –0.824 | 0.037 | 0.891 | 0.794 | 0.083 | 5.639 | 10 | >99.9% |
| <aa(G)> | –1.004 | 0.080 | 0.840 | 0.705 | 0.104 | 4.281 | 10 | >99.5% |
| <G> | –0.532 | 0.088 | 0.829 | 0.687 | 0.104 | 4.185 | 10 | >99.5% |
| <SSN> | –0.459 | 0.006 | 0.786 | 0.618 | 0.111 | 3.592 | 10 | >99% |
| <SSA> | –0.451 | 0.0004 | 0.772 | 0.596 | 0.121 | 3.443 | 10 | >99% |
| <aa(SSN)> | –0.785 | 0.058 | 0.744 | 0.554 | 0.126 | 3.127 | 10 | >98% |

| Lag 4, SC12–SC23 | | | | | | | | |
|---|---|---|---|---|---|---|---|---|
| Parameter | *a* | *b* | *r* | $r^2$ | *se* | *t* | *n* | *cl* |
| <aa(I:SSN)> | –0.793 | 0.096 | 0.856 | 0.733 | 0.151 | 5.258 | 12 | >99.9% |
| <aa(I:G)> | –0.772 | 0.088 | 0.830 | 0.690 | 0.164 | 4.677 | 12 | >99.9% |
| <aa> | –0.998 | 0.049 | 0.760 | 0.578 | 0.190 | 3.684 | 12 | >99.5% |
| <aa(G)> | –1.117 | 0.096 | 0.622 | 0.387 | 0.229 | 2.497 | 12 | >95% |
| <G> | –0.543 | 0.106 | 0.613 | 0.376 | 0.231 | 2.440 | 12 | >95% |
| <SSN> | –0.450 | 0.008 | 0.568 | 0.323 | 0.238 | 2.340 | 12 | >95% |
| <aa(SSN)> | –0.876 | 0.072 | 0.563 | 0.317 | 0.242 | 2.144 | 12 | >90% |
| <SSA> | –0.409 | 0.0004 | 0.514 | 0.264 | 0.254 | 1.689 | 12 | <90% |

| Lag 5, SC12–SC21 | | | | | | | | |
|---|---|---|---|---|---|---|---|---|
| Parameter | *a* | *b* | *r* | $r^2$ | *se* | *t* | *n* | *cl* |
| <aa(I:SSN)> | –0.672 | 0.075 | 0.969 | 0.939 | 0.048 | 10.944 | 10 | >99.9% |
| <aa(I:G)> | –0.638 | 0.067 | 0.898 | 0.806 | 0.085 | 5.753 | 10 | >99.9% |
| <aa> | –0.839 | 0.038 | 0.890 | 0.792 | 0.085 | 5.653 | 10 | >99.9% |
| <aa(G)> | –1.026 | 0.082 | 0.840 | 0.705 | 0.104 | 4.393 | 10 | >99.5% |
| <G> | –0.540 | 0.091 | 0.831 | 0.690 | 0.107 | 4.222 | 10 | >99.5% |
| <SSN> | –0.458 | 0.006 | 0.773 | 0.597 | 0.116 | 3.414 | 10 | >99% |
| <SSA> | –0.448 | 0.0004 | 0.757 | 0.573 | 0.127 | 3.282 | 10 | >98% |
| <aa(SSN)> | –0.787 | 0.058 | 0.731 | 0.534 | 0.129 | 3.048 | 10 | >98% |

| Lag 5, SC12–SC23 | | | | | | | | |
|---|---|---|---|---|---|---|---|---|
| Parameter | *a* | *b* | *r* | $r^2$ | *se* | *t* | *n* | *cl* |
| <aa(I:SSN)> | –0.805 | 0.098 | 0.865 | 0.748 | 0.149 | 5.433 | 12 | >99.9% |
| <aa(I:G)> | –0.776 | 0.090 | 0.831 | 0.690 | 0.164 | 4.560 | 12 | >99.9% |
| <aa> | –1.007 | 0.050 | 0.762 | 0.581 | 0.192 | 3.729 | 12 | >99.5% |
| <aa(G)> | –1.131 | 0.098 | 0.625 | 0.391 | 0.232 | 2.524 | 12 | >95% |
| <G> | –0.548 | 0.109 | 0.617 | 0.381 | 0.233 | 2.490 | 12 | >95% |
| <SSN> | –0.446 | 0.008 | 0.565 | 0.319 | 0.242 | 2.302 | 12 | >95% |
| <aa(SSN)> | –0.874 | 0.073 | 0.559 | 0.312 | 0.246 | 2.139 | 12 | >90% |
| <SSA> | –0.404 | 0.0004 | 0.510 | 0.260 | 0.259 | 1.656 | 12 | <90% |

Figure 11 displays the yearly variation of (a) AMO (1875–2012), (b) SOI (1875–2012), (c) NAO (1875–2012), (d) PDO (1900–2012), and (e) MLCO2 (1959–2012). The AMO is a fluctuation in the detrended sea surface temperature (SST) in the North Atlantic Ocean north of the equator (lat. 0°–70° N.).[75–79] The AMO has a cycle length of about 65–70 years, alternating between warm (positive) and cold (negative) phases believed to be associated with variations in the North Atlantic thermohaline circulation (THC), a density-driven global circulation pattern that involves the movement of warm equatorial surface waters to higher latitudes and the subsequent cooling and sinking of these waters into the deep ocean (also called the Atlantic Meridional Overturning Circulation; see <http://www.eoearth.org/view/article/150290>). The warm phase of the AMO appears to represent intervals of faster THC, while the cold phase appears to represent intervals of slower THC. The AMO index values are available online at <http://www.esrl.noaa.gov/psd/data/correlation/amon.us.long.data>.

The SOI describes the atmospheric response to anomalous changes in surface air pressure between Tahiti, French Polynesia, and Darwin, Australia, which generally varies inversely with the Oceanic Niño Index (ONI), an index that describes anomalous changes in SST in the Niño 3.4 region of the Pacific Ocean (located ±5° either side of the equator and ±25° either side of long. 145° W.).[80] Together, the variations in SOI and ONI often are used to describe the anomalous warming (El Niño) and cooling (La Niña) events associated with the El Niño Southern Oscillation (ENSO) pattern.[81] During warm events of the ENSO, the ONI ≥ 0.5 °C, and the SOI typically is ≤–8 for at least five consecutive months, while during cool events, the ONI ≤ –0.5 °C and SOI ≥ 8 for at least five consecutive months. Values of SOI (based on means and standard deviations over the period 1933–1992 inclusive) are available online at <http://www.bom.gov.au/climate/current/soihtml.shtml>.

The NAO describes the differences in surface air pressure between two widely separated locations, in particular Iceland and the subtropical Atlantic Ocean basin (e.g., the Azores, Portugal, or Gilbraltar).[82–85] The large-scale air mass movements described by the NAO controls the strength and direction of the westerly winds and storm tracks across the North Atlantic Ocean. During the positive phase of the NAO, there is a stronger subtropical high-pressure center and a deeper-than-usual Icelandic low, while during the negative phase, the opposite is true. Values for the NAO index are available online at <http://www.esrl.noaa.gov.psd/gcos_wgsp/Timeseries/Data/nao.long.data> and <http://www.cru.uea.ac.uk~timo/datapages/naoi.html>.

The PDO is defined as the leading principal component of the monthly SST anomalies in the North Pacific Ocean northward of lat. 20° N. The PDO fluctuates between warm (positive) and cool (negative) phases.[86–88] During the warm phase, the western Pacific Ocean surface waters become cool, and part of the eastern Pacific Ocean surface waters becomes warm, while during the cool phase, the opposite is true. Values of the PDO index are available online at <http://jisao.washington.edu/pdo/PDO.latest>.

The MLCO2 is a measure of the atmospheric concentration of $CO_2$ as measured at the Mauna Loa Observatory on the Big Island of Hawaii.[89–95] The observatory is located on the northern slope of the volcano Mauna Loa at an elevation of 3,400 m above sea level and 800 m below its summit. Annual means of MLCO2 (in units of ppm) are available online at <ftp://ftp.cmdl.noaa.gov/ccg/co2/trends/co2_annmean_mlo.txt>.

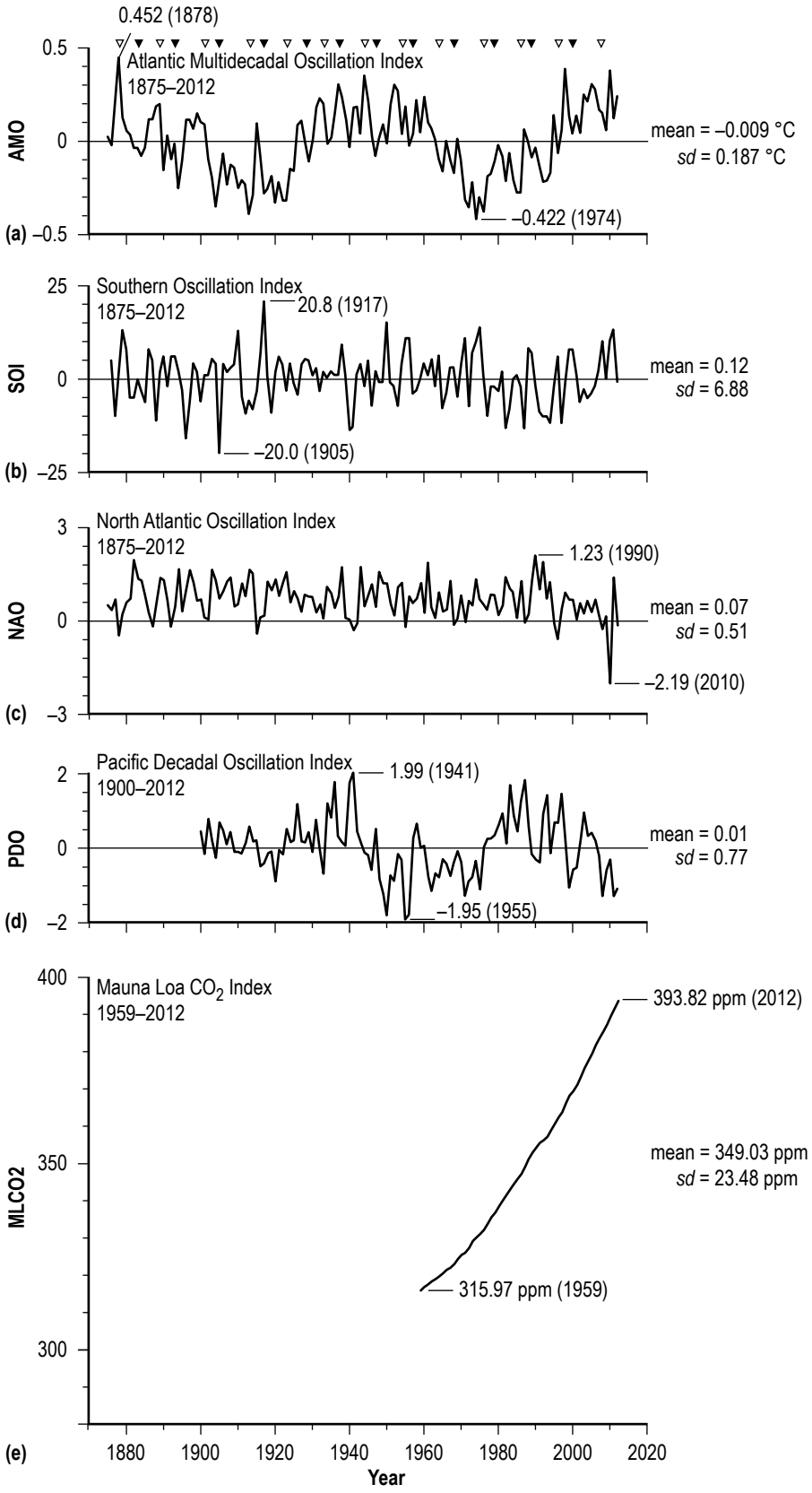


Figure 11. Annual variation of (a) AMO, (b) SOI, (c) NAO, (d) PDO, and (e) MLCO2.

Regarding the AMO, the highest value (to date) measures 0.452 °C in 1878, and the lowest value (to date) measures –0.422 °C in 1974. Overall, the long-term mean is –0.009 °C, having $sd = 0.187$ °C. Clearly, the AMO has been increasing in value (i.e., becoming more positive in value, indicating warming) since 1974, with all values since 1995 (except the value for 1996) being of positive value.

Regarding the SOI, the highest value (to date) measures 20.8 in 1917, and the lowest value (to date) measures –20 in 1905. Overall, the long-term mean is 0.12, having $sd = 6.88$.

Regarding the NAO, the highest value (to date) measures 1.23 in 1990, and the lowest value (to date) measures –2.19 in 2010. Overall, the long-term mean is 0.07, having $sd = 0.51$.

Regarding the PDO, the highest value (to date) measures 1.99 in 1941, and the lowest value (to date) measures –1.95 in 1955. Overall, the long-term mean is 0.01, having $sd = 0.77$.

Regarding the MLCO2, its values have consistently risen year to year from 315.97 ppm in 1959 to 393.82 ppm in 2012. The long-term mean measures 349.03 ppm, having $sd = 23.48$ ppm. Close inspection of the annual MLCO2 values reveals that not only is the atmospheric concentration of $CO_2$ increasing with the passage of time, but it is increasing at an accelerated rate (as placement of a straight edge along the curve clearly shows).

Table 3 gives the SC-length averages of each of the climatic parameters for SC12–SC23, and figure 12 displays them. For <AMO>, the warm phase is associated with SC12, SC16–SC18, and SC23, while the cool phase is associated with SC14, SC15, and SC20–SC22 (SC13 and SC16 appear to be cycles in transition). Since the warm phase is expected to persist at least three cycles in length, it is anticipated that SC24 and SC25 very likely will both be associated with the warm (positive) phase of the AMO as well. Interestingly, both the lows and highs of each individual phase appear to be increasing in value with the passage of time; i.e., SC23 (the current warm phase) is of higher positive value than SC18 (during the previous warm phase), which was higher than the value for SC12 (during the earliest warm phase). Similarly, the low of SC20 (during the just past cool phase) is higher than the low of SC15 (during the previous cool phase).

Regarding <SOI>, it appears that SC19 and SC20 were both associated with positive SOI, inferring cooler waters in the Niño 3.4 region (i.e., the likely occurrence of more La Niña-like conditions, on average), while SC21 and SC22 were both associated with negative SOI, inferring warmer waters in the Niño 3.4 region (i.e., the likely occurrence of more El Niño-like conditions, on average). SC20 is associated with the highest <SOI> (to date), while SC22 is associated with the lowest <SOI> (to date).

Regarding <NAO>, it has tended to be mostly of positive value. The highest positive value (to date) of <NAO> is associated with SC22, while the lowest value (to date) of <NAO> is associated with SC23. It is unclear whether SC24 will be of positive or negative <NAO> value.

Table 3. SC-length climate parametric mean values.

| Cycle | <AMO> | <SOI> | <NAO> | <PDO> | <MLCO2> |
|---|---|---|---|---|---|
| 12 | 0.087 | 0.58 | 0.03 | – | – |
| 13 | 0.013 | –0.49 | 0.25 | – | – |
| 14 | –0.168 | 0.24 | 0.23 | – | – |
| 15 | –0.225 | 1.48 | 0.22 | –0.06 | – |
| 16 | –0.012 | 1.06 | 0.11 | 0.33 | – |
| 17 | 0.126 | –0.43 | –0.004 | 0.72 | – |
| 18 | 0.137 | 0.16 | 0.22 | –0.61 | – |
| 19 | 0.094 | 2.63 | 0.09 | –0.58 | – |
| 20 | –0.184 | 2.73 | –0.05 | –0.64 | 325.10 |
| 21 | –0.170 | –3.43 | 0.05 | 0.54 | 339.19 |
| 22 | –0.091 | –4.60 | 0.30 | 0.55 | 354.42 |
| 23 | 0.164 | –0.73 | –0.21 | 0.17 | 372.82 |

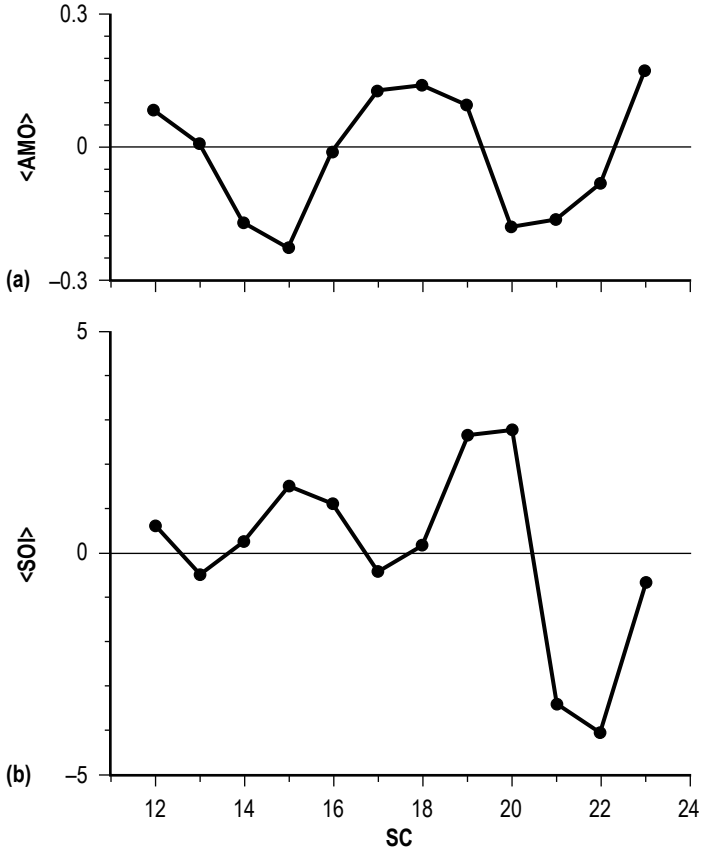


Figure 12. Variation of SC averages of (a) <AMO>, (b) <SOI>, (c) <NAO>, (d) <PDO>, and (e) <MLCO2>.

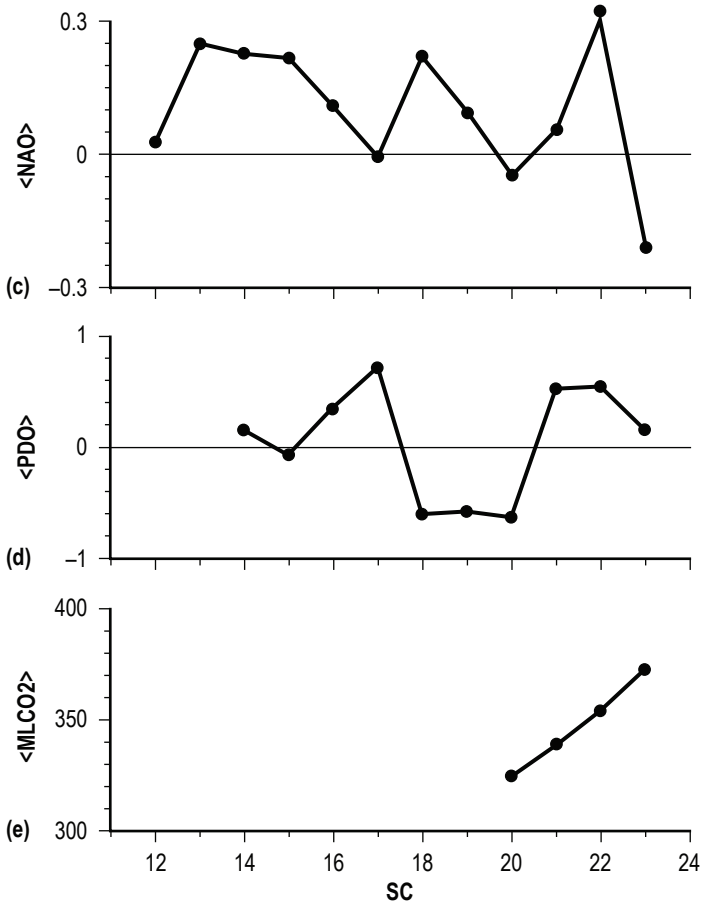


Figure 12. Variation of SC averages of (a) <AMO>, (b) SOI, (c) <NAO>, (d) <PDO>, and (e) <MLCO2> (Continued).

Regarding <PDO>, its highest positive value (to date) occurs in SC17, and its lowest negative value (to date) occurs in SC20. In appearance, its behavior looks similar to that of <AMO>, but of slightly different phase. Whereas the SC variation in <AMO> tends to have a smoother appearance, the SC variation in <PDO> is less smooth.

Regarding <MLCO2>, every cycle has a value that is higher than its preceding cyclic value. Hence, SC21 has a higher <MLCO2> than SC20, SC22 has a higher <MLCO2> than SC21, and SC23 has a higher <MLCO2> than SC22. Clearly, the expected value of <MLCO2> for SC24 is higher than that measured for SC23.

Figures 13a–e display scatter plots (for lag = 0–5 yr) of <GLOTI> versus <AMO>, <SOI>, <NAO>, <PDO>, and <MLCO2>, respectively. For <GLOTI> versus <AMO>, two inferred regressions are drawn, one for SC12–SC19 and the other for SC20–SC23. For <GLOTI> versus <MLCO2>, only the inferred regression for SC20–SC23 is drawn. The statistics for the inferred regressions are given in table 4.

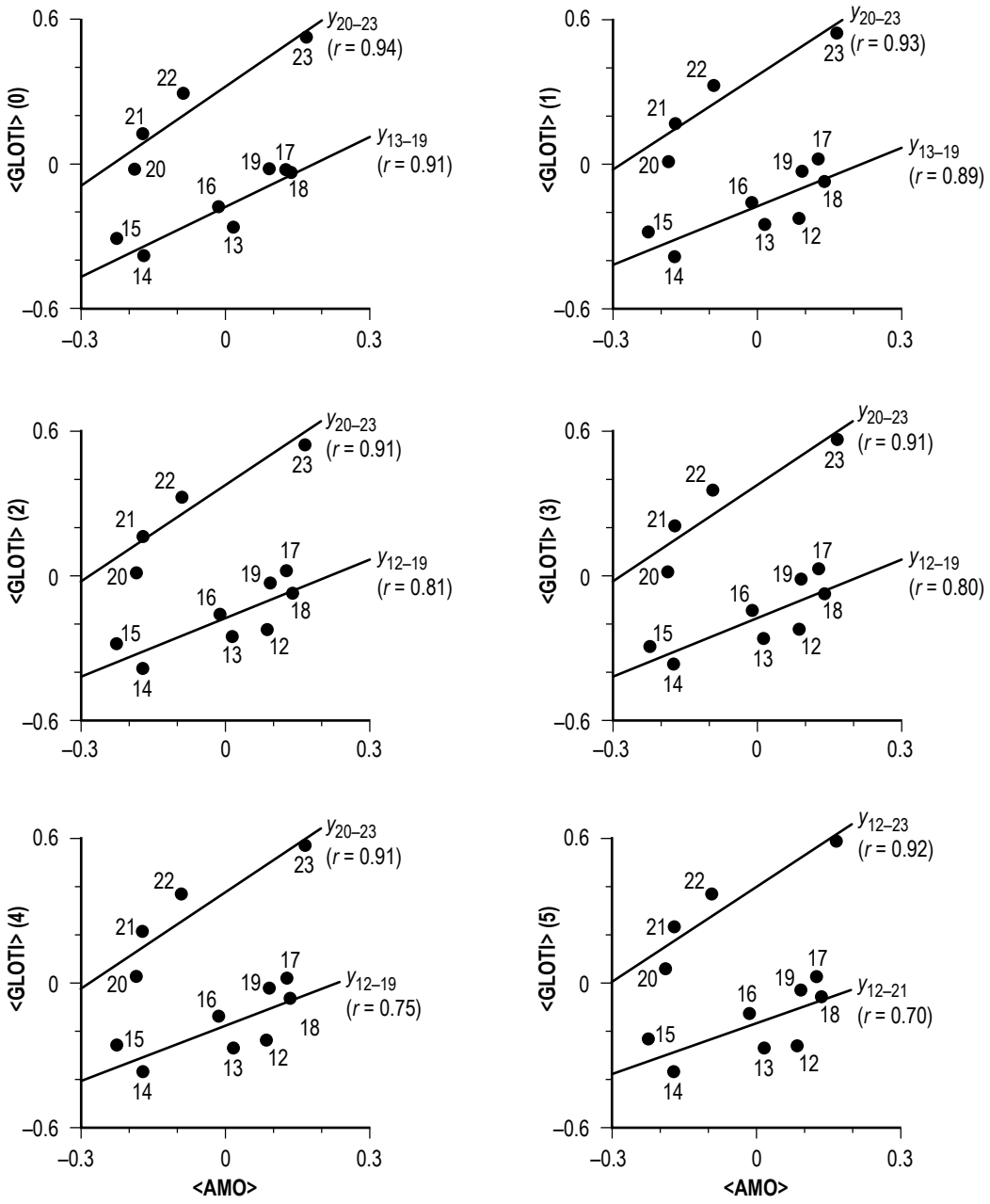


Figure 13a. Scatter plots of <GLOTI> versus <AMO> for lag 0–5 yr.

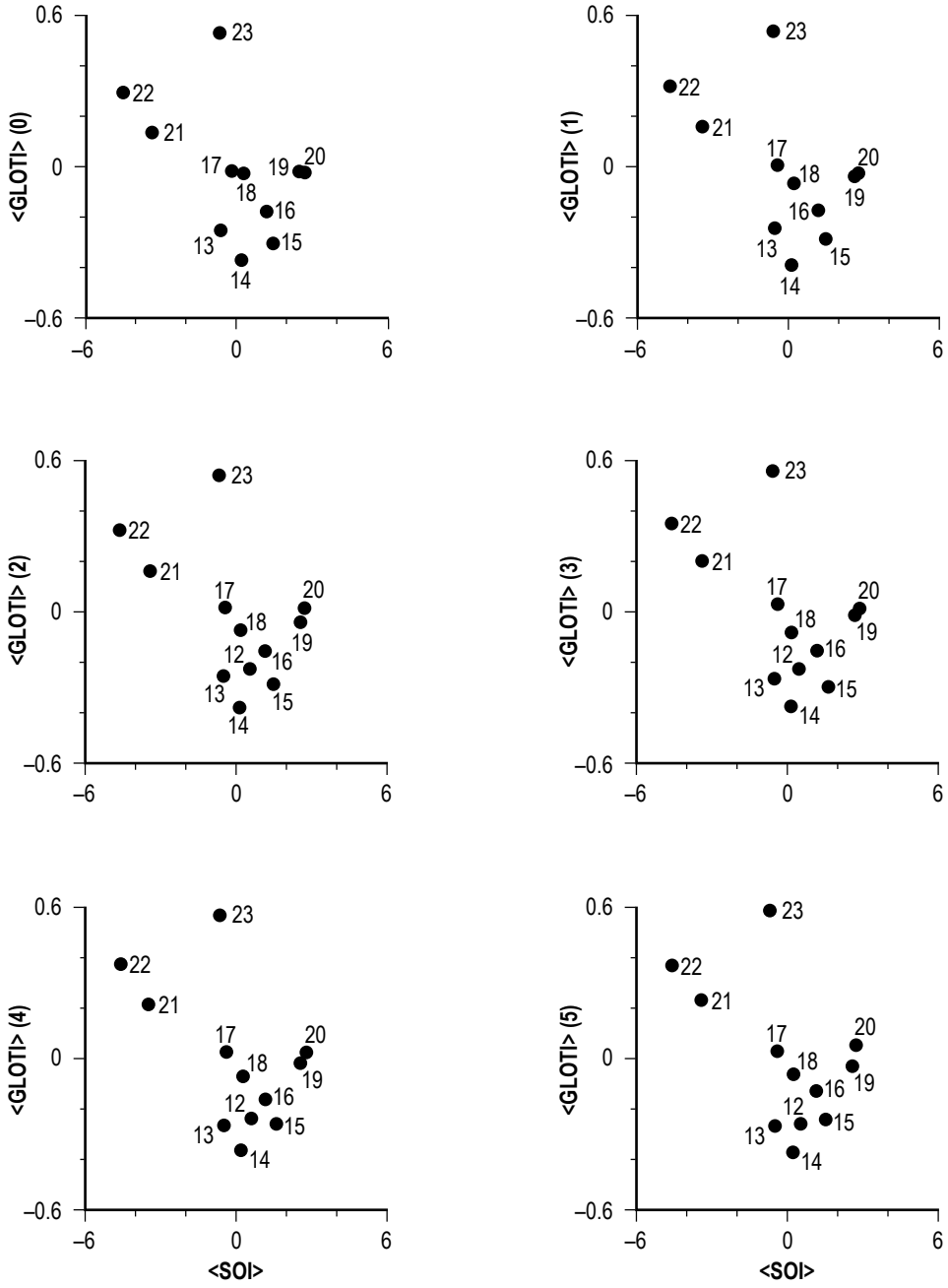


Figure 13b. Scatter plots of <GLOTI> versus <SOI> for lag 0–5 yr.

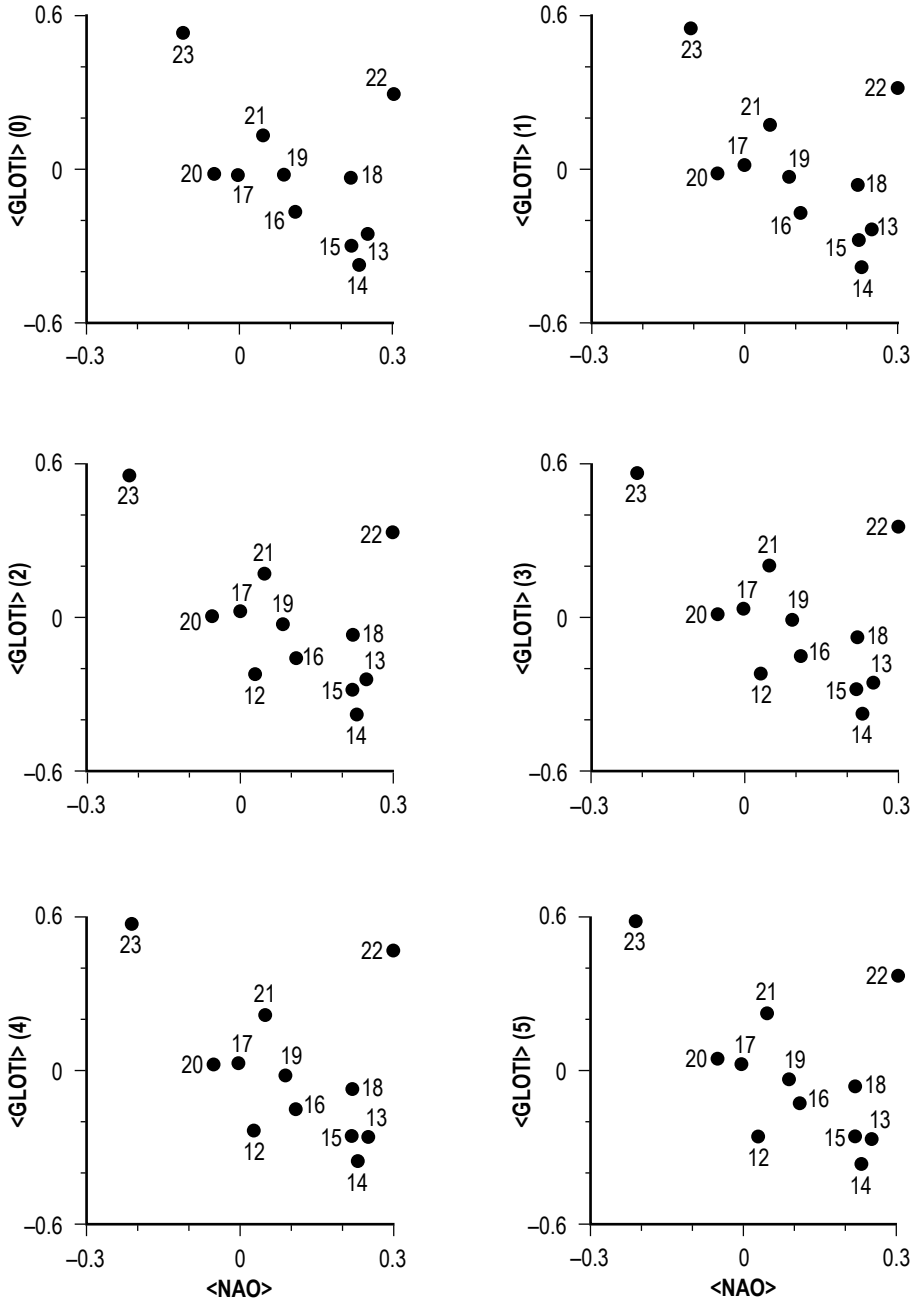


Figure 13c. Scatter plots of <GLOTI> versus <NAO> for lag 0–5 yr.

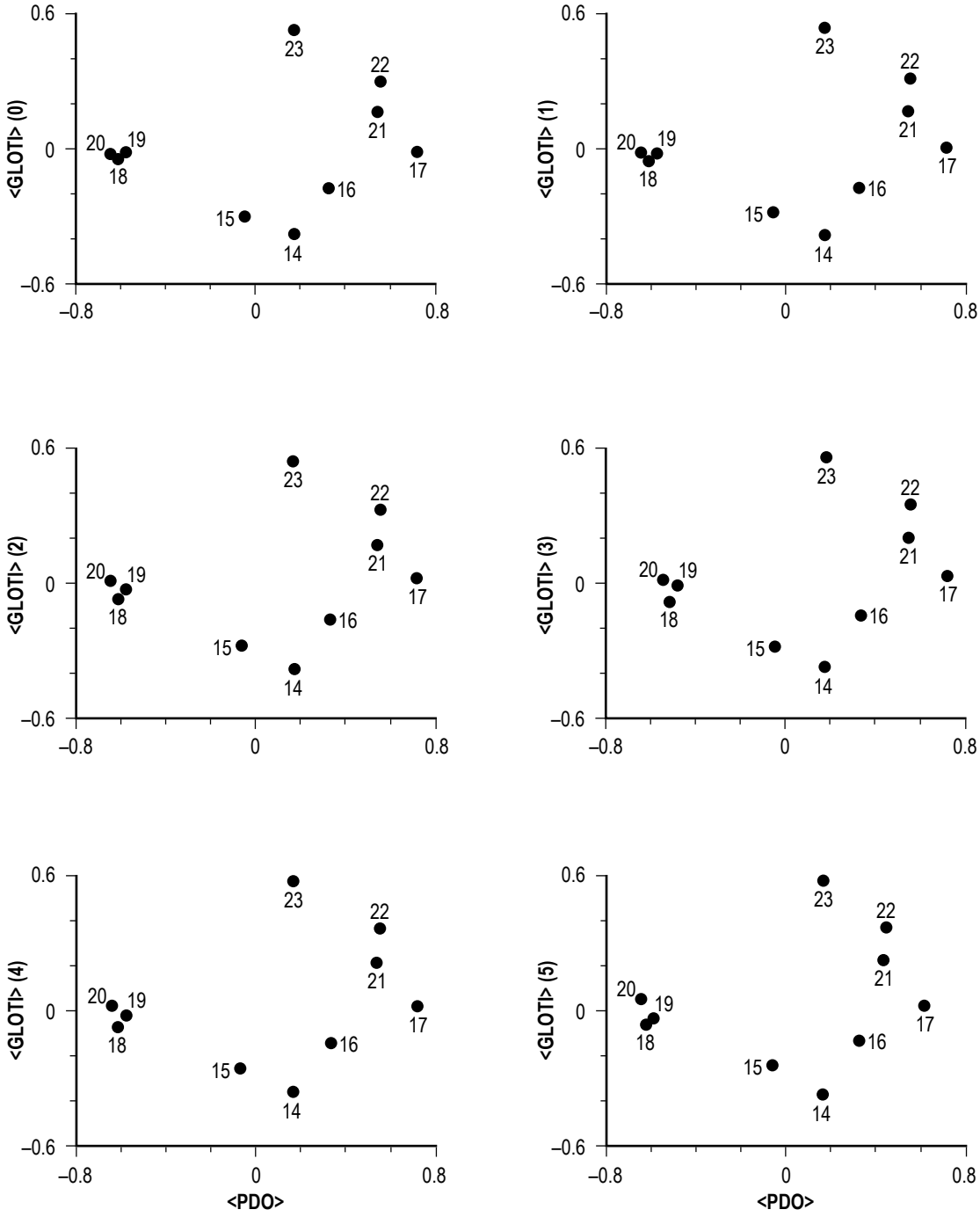


Figure 13d. Scatter plots of <GLOTI> versus <PDO> for lag 0–5 yr.

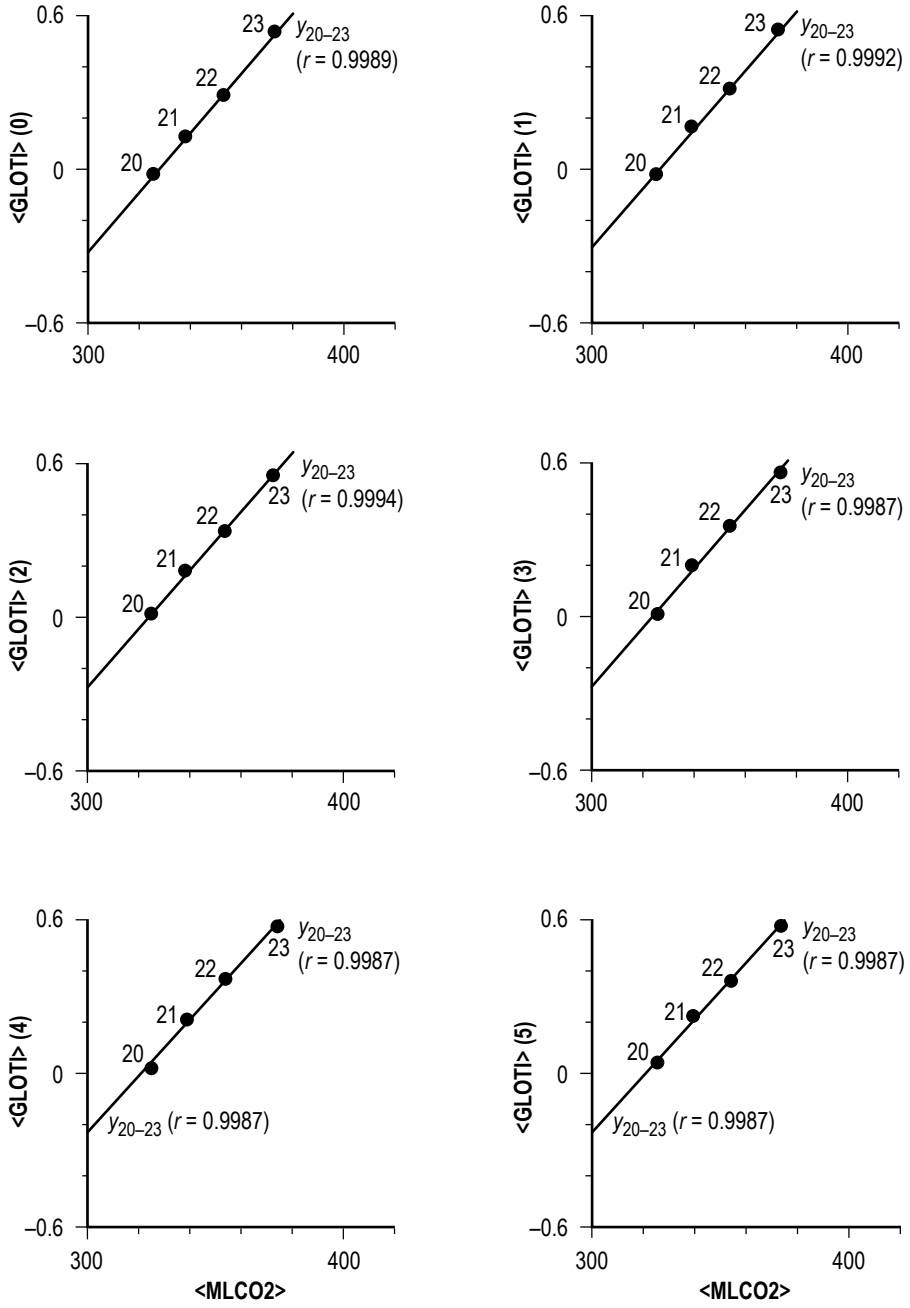


Figure 13e. Scatter plots of <GLOTI> versus <MLCO2> for lag 0–5 yr.

Table 4. Correlations of SC-length averages of GLOTI against SC averages of selected climate parameters.

| Lag 0, SC13–SC19 | | | | | | | | |
|---|---|---|---|---|---|---|---|---|
| Parameter | *a* | *b* | *r* | $r^2$ | *se* | *t* | *n* | *cl* |
| <AMO> | –0.161 | 0.925 | 0.910 | 0.828 | 0.066 | 4.895 | 7 | >99.5% |

| Lag 0, SC20–SC23 (*n* = 4) | | | | | | | |
|---|---|---|---|---|---|---|---|
| Parameter | *a* | *b* | *r* | $r^2$ | *se* | *t* | *cl* |
| <MLCO2> | –3.756299 | 0.011460 | 0.9989 | 0.9978 | 0.015 | 27.666 | >99.8% |
| <AMO> | 0.326654 | 1.368739 | 0.9401 | 0.8838 | 0.098 | 3.900 | >90% |

| Lag 1, SC13–SC19 | | | | | | | | |
|---|---|---|---|---|---|---|---|---|
| Parameter | *a* | *b* | *r* | $r^2$ | *se* | *t* | *n* | *cl* |
| <AMO> | –0.160 | 0.925 | 0.890 | 0.793 | 0.074 | 4.362 | 7 | >99% |

| Lag 1, SC20–SC23 (*n* = 4) | | | | | | | |
|---|---|---|---|---|---|---|---|
| Parameter | *a* | *b* | *r* | $r^2$ | *se* | *t* | *cl* |
| <MLCO2> | –3.753224 | 0.011498 | 0.9992 | 0.9984 | 0.012 | 34.075 | >99.9% |
| <AMO> | 0.342169 | 1.358281 | 0.9301 | 0.8652 | 0.106 | 3.582 | >90% |

| Lag 2, SC12–SC19 | | | | | | | | |
|---|---|---|---|---|---|---|---|---|
| Parameter | *a* | *b* | *r* | $r^2$ | *se* | *t* | *n* | *cl* |
| <AMO> | –0.176 | 0.827 | 0.810 | 0.657 | 0.088 | 3.389 | 8 | >99% |

| Lag 2, SC20–SC23 (*n* = 4) | | | | | | | |
|---|---|---|---|---|---|---|---|
| Parameter | *a* | *b* | *r* | $r^2$ | *se* | *t* | *cl* |
| <MLCO2> | –3.683248 | 0.011342 | 0.9994 | 0.9988 | 0.012 | 34.964 | >99.9% |
| <AMO> | 0.356746 | 1.341576 | 0.9315 | 0.8677 | 0.104 | 3.6221 | >90% |

| Lag 3, SC12–SC19 | | | | | | | | |
|---|---|---|---|---|---|---|---|---|
| Parameter | *a* | *b* | *r* | $r^2$ | *se* | *t* | *n* | *cl* |
| <AMO> | –0.174 | 0.815 | 0.796 | 0.633 | 0.091 | 3.220 | 8 | >98% |

| Lag 3, SC20–SC23 (*n* = 4) | | | | | | | |
|---|---|---|---|---|---|---|---|
| Parameter | *a* | *b* | *r* | $r^2$ | *se* | *t* | *cl* |
| <MLCO2> | –3.621020 | 0.011211 | 0.9987 | 0.9975 | 0.017 | 23.335 | >99.8% |
| <AMO> | 0.370436 | 1.298026 | 0.9112 | 0.8303 | 0.116 | 3.128 | >90% |

| Lag 4, SC12–SC19 | | | | | | | | |
|---|---|---|---|---|---|---|---|---|
| Parameter | *a* | *b* | *r* | $r^2$ | *se* | *t* | *n* | *cl* |
| <AMO> | –0.173 | 0.747 | 0.748 | 0.559 | 0.098 | 2.757 | 8 | >95% |

| Lag 4, SC20–SC23 (*n* = 4) | | | | | | | |
|---|---|---|---|---|---|---|---|
| Parameter | *a* | *b* | *r* | $r^2$ | *se* | *t* | *cl* |
| <MLCO2> | –3.628428 | 0.011270 | 0.9987 | 0.9975 | 0.015 | 26.391 | >99.8% |
| <AMO> | 0.383674 | 1.301415 | 0.9088 | 0.8259 | 0.118 | 3.080 | >90% |

| Lag 5, SC12–SC19 | | | | | | | | |
|---|---|---|---|---|---|---|---|---|
| Parameter | *a* | *b* | *r* | $r^2$ | *se* | *t* | *n* | *cl* |
| <AMO> | –0.170 | 0.711 | 0.702 | 0.493 | 0.106 | 2.426 | 8 | >90% |

| Lag 5, SC20–SC23 (*n* = 4) | | | | | | | |
|---|---|---|---|---|---|---|---|
| Parameter | *a* | *b* | *r* | $r^2$ | *se* | *t* | *cl* |
| <MLCO2> | –3.530094 | 0.011028 | 0.9987 | 0.9974 | 0.012 | 33.618 | >99.9% |
| <AMO> | 0.396926 | 1.290762 | 0.9211 | 0.8485 | 0.108 | 3.347 | >90% |

For the interval SC20–SC23, clearly, the strongest inferred regressions are those between <GLOTI> and <MLCO2>, having $cl > 99.8\%$ and >99.9%, and $se = 0.01$ °C. This suggests that one might be able to better estimate <GLOTI> for the current ongoing SC24, and perhaps future SC25 and beyond (presuming the validity of the fit), on the basis of having accurate estimates of <MLCO2> for these cycles.

From figure 12 (and table 3), it is clear that <MLCO2> is increasing over time. A simple linear fit of <MLCO2> versus SC yields $y = 7.344 + 15.839x$, where $y$ refers to <MLCO2> and $x$ refers to the SC. The inferred regression has $r = 0.99807$, $r^2 = 0.99615$, $se = 1.557$, $t = 22.74$, and $cl > 99.8\%$. Presuming the validity of the fit, one estimates the <MLCO2> for SC24 and SC25, respectively, to be $387.48 \pm 1.56$ ppm and $403.32 \pm 1.56$ ppm ($\pm 1$ *se* prediction interval). Applying these values in the inferred linear regressions (dependent upon selection of lag) results in <GLOTI> $= 0.68 \pm 0.02$ °C for SC24 (lag = 0 yr) to $0.74 \pm 0.01$ °C (lag = 5 yr) and <GLOTI> $= 0.87 \pm 0.02$ °C for SC25 (lag = 0 yr) to $0.92 \pm 0.01$ °C (lag = 5 yr). Hence, the projected <GLOTI> for SC24 appears very likely to be higher than that measured for SC23; namely, <GLOTI> > 0.526 °C (lag = 0 yr) for SC24. If true, then this finding contradicts the prediction of Solheim et al.,[96,97] who suggest that the <GLOTI> will be much cooler for SC24 as compared to SC23, a prediction based on the ongoing declining solar activity and the long duration of SC23.

Figure 14 compares annual values of the GLOTI for SC23 and SC24 for similar phasing (i.e., the elapsed time in years $t$ from Emin). Plainly, the GLOTI measured during SC24 (2008–2012) has been higher every year than was seen for similar phasing in SC23, suggesting that, indeed, the <GLOTI> for SC24 will be higher than was measured for SC23 (0.526 °C).

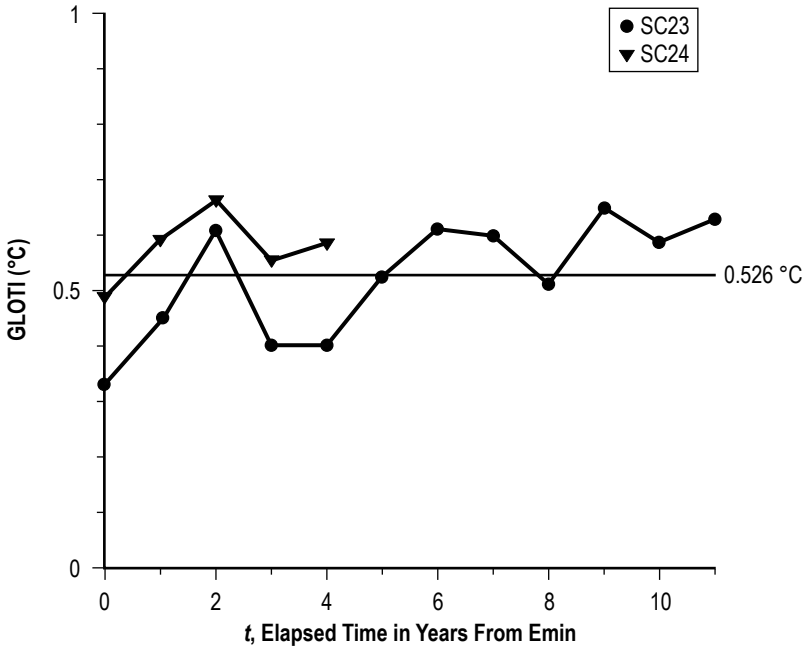


Figure 14. Annual variation of GLOTI for SC23 (filled circles) and SC24 (filled triangles) for similar phasing.

## 3. DISCUSSION AND SUMMARY

This TP has examined SC-length averages of the January–December values of the GLOTI in relation to SC-length averages of various annual values of descriptors of solar-geomagnetic activity and climate, incorporating lags of 0–5 yr. For the interval SC12–SC21, the best inferred linear correlation is the one found between <GLOTI> and <aa(I:SSN)>, incorporating lag = 5 yr and having $r = 0.969$ and $se = 0.048$ °C. The descriptor <aa(I:SSN)> is a proxy for the strength of the recurrent, long-lived events, like coronal holes, which tend to be more prevalent during the decline of the SC between cycle maximum amplitude and next SC minimum amplitude. For the interval SC20–SC23, the best inferred linear correlation is the one found between <GLOTI> and <MLCO2>, incorporating lag = 2 yr and having $r = 0.9994$ and $se = 0.012$ °C. A comparison of <GLOTI> and <SSN> for SC12–SC21 shows that its best correlation is for lag = 0 yr, having $r = 0.831$ and $se = 0.093$ °C, a result that contrasts that found by Stauning, who reports the best correlation to be the one incorporating lag = 3 yr.[62] Since the global temperature values (i.e., the GLOTI) are found to change slightly from year to year, it might be that this slight variation in their determination and the use of a slightly longer database (2–3 yr longer) used in the present study can account for the difference in the fits (i.e., best fit being lag = 0 yr versus lag = 3 yr). For the overall interval SC12–SC23, the correlation between <GLOTI> and <SSN> weakens considerably, having $r < 0.57$ and $se > 0.23$ °C for all lags 0–5 yr. Hence, SC22 (1986–1995) and SC23 (1996–2007) appear to be statistical outliers with respect to the inferred preferential linear relationship found between <GLOTI> and SC-length averages of solar-geomagnetic activity descriptors based on SC12–SC21. Recall that both GLOTI and <GLOTI> continue to rise (through SC23), while solar activity appears to be waning, suggesting that something other than solar-geomagnetic activity must now be responsible for the continued rise of global temperatures, especially since SC20.

Based on the inferred preferential linear correlation found between <MLCO2> and SC for SC20–SC23, having $r = 0.998$ and $se = 1.56$ ppm, one estimates <MLCO2> for SC24 to be about $387.48 \pm 1.56$ (the $\pm 1$ *se* prediction interval). Using this estimate (and lag = 2 yr) for <MLCO2>, one further predicts <GLOTI> $= 0.71 \pm 0.02$ °C for SC24, a value considerably larger than that seen for SC23 (0.551 °C for lag 2 yr). Hence, based on this analysis and assuming the validity of the inferred preferential linear correlation, one expects <GLOTI> to continue to rise in SC24 and to be warmer than was seen in SC23, a result in contrast to that given by Solheim et al.,[96,97] who suggest that <GLOTI> will instead be much cooler for SC24 as compared to SC23, a prediction based on the declining levels of solar activity and long duration of SC23. (Based on extrapolated levels of <MLCO2>, one expects <GLOTI> to exceed 1 °C in SC26, its expected onset about 2030–2032.)

Now, while solar irradiance has been found to vary with solar activity[98–105] (i.e., over the SC), it cannot account for the observed continued warming evident in <GLOTI>, especially since SC20. Nor can climate factors, such as the AMO, SOI, NAO, or PDO, account for the continuing increase in <GLOTI> that is currently being experienced. Instead, it appears that increased levels of greenhouse gases[106–109] must be the underlying cause for the continued warming that has occurred, especially over the past 50 years or so (i.e., since onset for SC20).

Figure 15 compares (a) GLOTI, (b) aa(SSN) and aa(I:SSN), (c) the annual greenhouse gases index (AGGI), and (d) the global radiative forcing of $CO_2$, methane ($CH_4$), nitrous oxide ($NO_2$), and total greenhouse gases for the interval 1979–2012 (available online at <http://www.esrl.noaa.gov/gmd/aggi/aggi.html>). Plainly, while the GLOTI is rising (in particular since 1985, with year-to-year variations of ±0.21 °C or less) during the interval 1979–2012, the overall cyclic variation of solar-geomagnetic activity (i.e., aa(SSN) and aa(I:SSN)) is now declining, and greenhouse gas radiative forcing is continuously rising. The decreasing solar-geomagnetic activity suggests that the Sun's total irradiance must also be declining, while the increase in greenhouse gases suggests that more heat is being trapped than is being reradiated back into space. In particular, the GLOTI is found to correlate strongly with the AGGI, the total radiative forcing of greenhouse gases and the radiative forcing of $CO_2$ (the chief contributor to the radiative forcing of greenhouse gases: >64% in 2012). For GLOTI versus AGGI, the inferred regression is $y = -0.691 + 1.014x$, having $r = 0.875$, $r^2 = 0.765$, $se = 0.09$, $t = 10.096$, and $cl > 99.9\%$. For GLOTI versus the total radiative forcing of greenhouse gases, the inferred regression is $y = -0.691 + 0.466x$, having $r = 0.874$, $r^2 = 0.765$, $se = 0.09$, $t = 10.405$, and $cl > 99.9\%$. For GLOTI versus the radiative forcing of $CO_2$, the inferred regression is $y = -0.535 + 0.653x$, having $r = 0.878$, $r^2 = 0.771$, $se = 0.09$, $t = 10.597$, and $cl > 99.9\%$.

In conclusion, the inferred preferential linear relationship between <GLOTI> and SC-length averages of solar-geomagnetic activity that was apparent prior to SC21 (onset 1986) no longer appears to be the dominate factor once it was in the ongoing warming expressed by <GLOTI>. Instead, it is the increase in greenhouse gases (primarily $CO_2$) that better correlates with the increase in <GLOTI>, in particular since SC20.

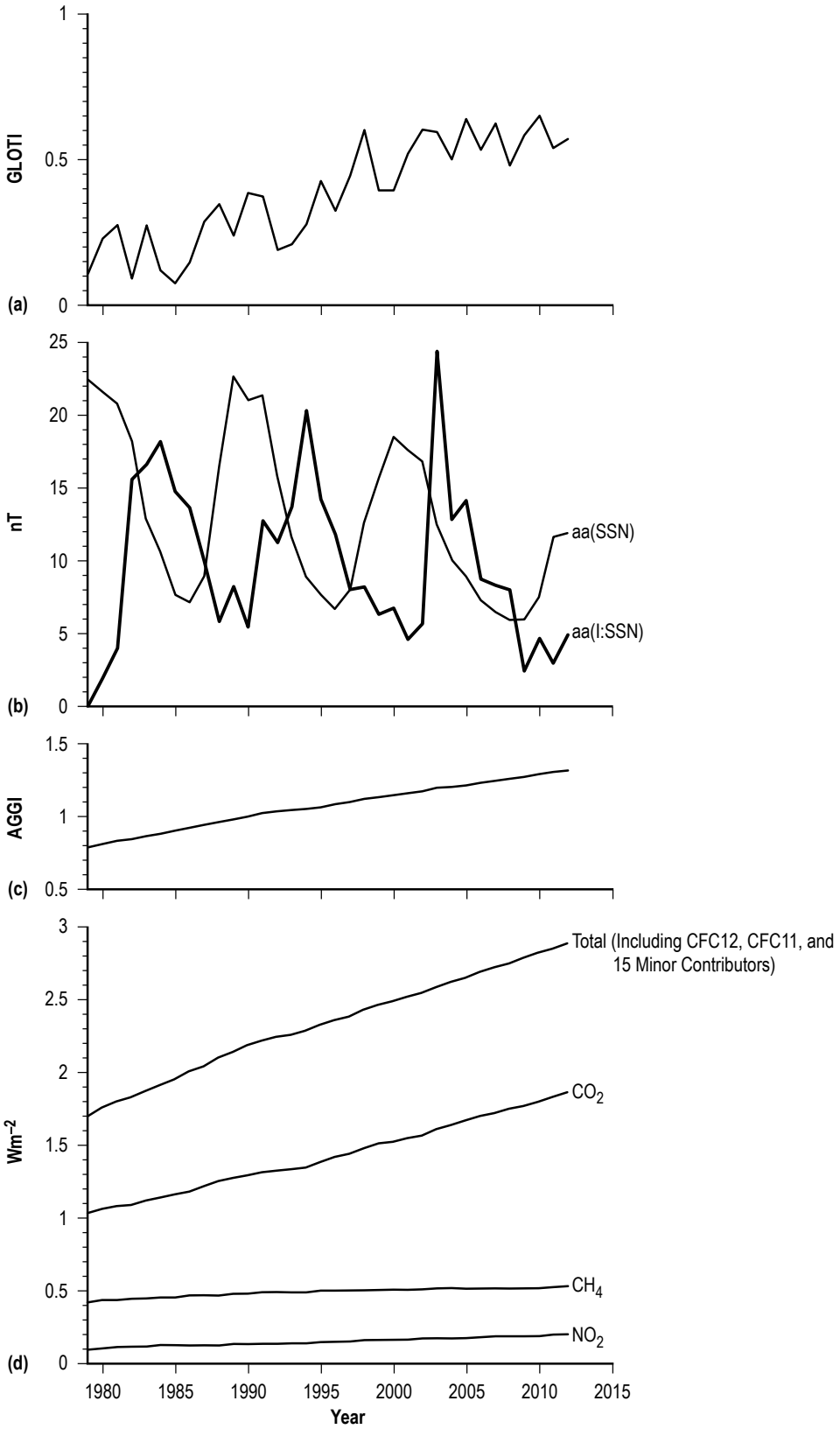


Figure 15. Annual variation of (a) GLOTI, (b) aa(SSN) and aa(I:SSN), (c) the AGGI, and (d) the radiative forcing of $NO_2$, $CH_4$, $CO_2$, and total (including CFC12, CFC11, and 15 minor contributors) for the interval 1979–2012.

## REFERENCES


1. Wilcox, J.M.: "Solar activity and the weather," *J. Atmos. Terr. Phys.*, Vol. 37, No. 2, pp. 237–256, doi:10.1016/0021-9169(75)90108-7, February 1975.

2. Dickinson, R.E.: "Solar Variability and the Lower Atmosphere," *Bull. Am. Meterol. Soc.*, Vol. 56, No. 12, pp. 1240–1248, doi:10.1175/1520-0477(1975)056<1240:SVATLA>2.0.CO;2, December 1975.

3. Herman, J.R.; and Goldberg, R.A.: *Sun*, *Weather*, *and Climate*, NASA SP-426, NASA Headquarters, Washington, DC, 360 pp., 1978.

4. Pittock, A.B.: "A critical look at long-term Sun-weather relationships," *Rev. Geophys.*, Vol. 16, No. 3, pp. 400–420, doi:10.1029/RG016i003p00400, August 1978.

5. Reid, G.C.: "Solar total irradiance variations and the global sea surface temperature record," *J. Geophys. Res.-Atmos.*, Vol. 96, No. D2, pp. 2835–2844, doi:10.1029/90JD02274, February 1991.

6. Friis-Christensen, E.; and Lassen, K.: "Length of the Solar Cycle: An Indicator of Solar Activity Closely Associated with Climate," *Science*, Vol. 254, No. 5032, pp. 698–700, doi:10.1126/science.254.5032.698, November 1991.

7. Lassen, K.; and Friis-Christensen, E.: "Variability of the solar cycle length during the past five centuries and the apparent association with terrestrial climate," *J. Atmos. Sol.-Terr. Phys.*, Vol. 57, No. 8, pp. 835–845, doi:10.1016/0021-9169(94)00088-6, July 1995.

8. Lean, J.; Beer, J.; and Bradley, R.: "Reconstruction of solar irradiance since 1610: Implications for climate change," *Geophys. Res. Lett.*, Vol. 22, No. 23, pp. 3195–3198, doi:10.1029/95GL03093, December 1995.

9. Soon, W.H.; Posmentier, E.S.; and Baliunas, S.L.: "Inference of Solar Irradiance Variability from Terrestrial Temperature Changes, 1880–1993: an Astrophysical Application of the Sun-Climate Connection," *Astrophys. J.*, Vol. 472, pp. 891–902, doi:10.1086/178119, December 1996.

10. Svensmark, H.; and Friis-Christensen, E.; "Variation of cosmic ray flux and global cloud coverage–a missing link in solar-climate relationships," *J. Atmos. Sol.-Terr. Phys.*, Vol. 59, No. 11, pp. 1225–1232, doi:10.1016/s1364-6826(97)00001-1, January 1997.

11. Reid, G.C.: "Solar Forcing of Global Climate Change since the Mid-17th Century," *Clim. Change*, Vol. 37, No. 2, pp. 391–405, doi:10.1023/A:1005307009726, October 1997.

12. Hoyt, D.V.; and Schatten, K.H.: *The Role of the Sun in Climate Change*, Oxford University Press, New York, NY, 288 pp., 1997.

13. Solanki, S.K.; and Fligge, M.: "Solar irradiance since 1874 revisited," *Geophys. Res. Lett.*, Vol. 25, No. 3, pp. 341–344, doi:10.1029/98GL50038, February 1998.

14. Cliver, E.W.; Boriakoff, V.; and Feynman, J.: "Solar variability and climate change: Geomagnetic aa index and global surface temperature," *Geophys. Res. Lett.*, Vol. 25, No. 7, pp. 1035–1038, doi:10.1029/98GL00499, April 1998.

15. Fröhlich, C.; and Lean, J.: "The Sun's total irradiance: Cycles, trends, and related climate change uncertainties since 1976," *Geophys. Res. Lett.*, Vol. 25, No. 23, pp. 4377–4380, doi:10.1029/1998GL900157, December 1998.

16. van Geel, B.; Raspopov, O.M.; Renssen, H.; et al.: "The role of solar forcing upon climate change," *Quaternary Sci. Rev.*, Vol. 18, No. 3, pp. 331–338, doi:10.1016/S0277-3791(98)00088-2, March 1999.

17. Kernthaler, S.C.; Toumi, R.; and Haigh, J.D.: "Some doubts concerning a link between cosmic ray fluxes and global cloudiness," *Geophys. Res. Lett.*, Vol. 26, No. 7, pp. 863–865, doi:10.1029/1999GL900121, April 1999.

18. Rycroft, M.J.; Israelsson, S.; and Price, C.: "The global atmospheric electric circuit, solar activity and climate change," *J. Atmos. Sol.-Terr. Phys.*, Vol. 62, Nos. 17–18, pp. 1563–1576, doi:10.1016/S1364-6826(00)00112-7, November 2000.

19. Svensmark, H.: "Cosmic Rays and Earth's Climate," *Space Sci. Rev.*, Vol. 93, Nos. 1–2, pp. 175–185, doi:10.1023/A:1026592411634, July 2000.

20. Beer, J.; Mende, W.; and Stellmacher, R.: "The role of the sun in climate forcing," *Quaternary Sci. Rev.*, Vol. 19, Nos. 1–5, pp. 403–415, January 2000.

21. Renssen, H.; van Geel, B.; van der Plicht, J.; and Magny, M.: "Reduced solar activity as a trigger for the start of the Younger Dryas?" *Quaternary Int.*, Vols. 68–71, pp. 373–383, doi:10.1016/S1040-6182(00)00060-4, June 2000.

22. Reid, G.C.: "Solar Variability and the Earth's Climate: Introduction and Overview," *Space Sci. Rev.*, Vol. 94, Nos. 1–2, pp. 1–11, doi:10.1023/A:1026797127105, November 2000.

23. Marsh, N.; and Svensmark, H.: "Cosmic Rays, Clouds, and Climate," *Space Sci. Rev.*, Vol. 94, No. 1, pp. 215–230, doi:10.1023/A:1026723423896, October 2000.

24. Tinsley, B.A.: "Influence of Solar Wind on the Global Electric Circuit, and Inferred Effects on Cloud Microphysics, Temperature, and Dynamics in the Troposphere," *Space Sci. Rev.*, Vol. 94, Nos. 1–2, pp. 231–258, doi:10.1023/A:1026775408875, November 2000.

25. Soon, W.; Baliunas, S.; Posmentier, E.S.; and Okeke, P.: "Variations of solar coronal hole area and terrestrial lower tropospheric air temperature from 1979 to mid-1998: astronomical forcings of change in earth's climate?" *New Astron.*, Vol. 4, No. 8, pp. 563–579, doi:10.1016/S1384-1076(00)00002-6, January 2000.

26. Tobias, S.M.; and Weiss, N.O.: "Resonant Interactions between Solar Activity and Climate," *J. Climate*, Vol. 13, No. 21, pp. 3745–3759, doi:10.1175/1520-0442(2000)0132.0.CO;2, November 2000.

27. Douglass, D.H.; and Clader, B.D.: "Climate sensitivity of the Earth to solar irradiance," *Geophys. Res. Lett.*, Vol. 29, No. 16, 4 pp., doi:10.1029/2002GL015345, August 2002.

28. Lean, J.L.; Wang, Y.-M.; and Sheeley Jr., N.R.: "The effect of increasing solar activity on the Sun's total and open magnetic flux during multiple cycles: Implications for solar forcing of climate," *Geophys. Res. Lett.*, Vol. 29, No. 24, 4 pp., doi:10.1029/2002GL015880, December 2002.

29. Rind, D.: "The Sun's Role in Climate Variations," *Science*, Vol. 296, pp. 673–677, doi:10.1126/science.1069562, April 2002.

30. Sharma, M.: "Variations in solar magnetic activity during the last 200,000 Years: is there a Sun-climate connection?" *Earth Planet. Sci. Lett.*, Vol. 199, Nos. 3–4, pp. 459–472, doi:10.1016/S0012-821X(02)00516-2, June 2002.

31. Kristjánsson, J.E.; Staple, A.; Kristiansen, J.; and Kaas, E.: "A new look at possible connections between solar activity, clouds and climate," *Geophys. Res. Lett.*, Vol. 29, No. 23, 4 pp., doi:10.1029/2002GL015646, December 2002.

32. Marsh, N.; and Svensmark, H.: "Solar Influence on Earth's Climate," *Space Sci. Rev.*, Vol. 107, Nos. 1–2, pp. 317–325, doi:10.1023/A:1025573117134, April 2003.

33. Gleisner, H.; and Thejll, P.: "Patterns of tropospheric response to solar variability," *Geophys. Res. Lett.*, Vol. 30, No. 13, 4 pp., doi:10.1029/2003GL017129, July 2003.

34. Tsiropoula, G.: "Signatures of solar activity variability in meteorological parameters," *J. Atmos. Solar-Terr. Phys.*, Vol. 65, No. 4, pp. 469–482, doi:10.1016/S1364-6826(02)00295-X, March 2003.

35. Haigh, J.D.: "The Effects of Solar Variability on the Earth's Climate," *Philos. T. R. Soc. Lon. A*, Vol. 361, No. 1802, pp. 95–111, doi:10.1098/rsta.2002.1111, January 2003.

36. Laut, P.: "Solar activity and terrestrial climate: an analysis of some purported correlations," *J. Atmos. Sol.-Terr. Phys.*, Vol. 65, No. 7, pp. 801–812, doi:10.1016/S1364-6826(03)00041-5, January 2003.

37. Kristjánsson, J.E.; Kristiansen, J.; and Kaas, E.: "Solar activity, cosmic rays, clouds and climate—an update," *Adv. Space Res.*, Vol. 34, No. 2, pp. 407–415, doi:10.1016/j.asr.2003.02.040, February 2004.

38. Raspopov, O.M.; Dergachev, V.A.; and Kolström, T.: "Hale Cyclicity of Solar Activity and Its Relation to Climate Variability," *Sol. Phys.*, Vol. 224, No. 1, pp. 455–463, doi:10.1007/s11207-005-5251-8, September 2004.

39. Harrison, R.G.: "The Global Atmospheric Electrical Circuit and Climate," *Sur. Geophys.*, Vol. 25, Nos. 5–6, pp. 441–484, doi:10.1007/s10712-004-5439-8, November 2004.

40. Ponyavin, D.I.: "Solar Cycle Signal in Geomagnetic Activity and Climate," *Sol. Phys.*, Vol. 224, Nos. 1–2, pp. 465–471, doi:10.1007/s11207-005-4979-5, October 2004.

41. de Jager, C.: "Solar Forcing of Climate. 1: Solar Variability," *Space Sci. Rev.*, Vol. 120, Nos. 3–4, pp. 197–241, doi:10.1007/s11214-005-7046-5, October 2005.

42. Versteegh, G.J.M.: "Solar Forcing of Climate. 2: Evidence from the Past," *Space Sci. Rev.*, Vol. 120, Nos. 3–4, pp. 243–286, doi: 10.1007/s11214-005-7047-4, October 2005.

43. Bard, E.; and Frank, M.: "Climate change and solar variability: What's new under the Sun?" *Earth Planet. Sci. Lett.*, Vol. 248, Nos. 1–2, pp. 1–14, doi:10.1016/j.epsl.2006.06.016, August 2006.

44. Foukal, P.; Fröhlich, C.; Spruit, H.; and Wigley, T.M.L.: "Variations in solar luminosity and their effect on the Earth's climate," *Nature*, Vol. 443, No. 5072, pp. 161–166, doi:10.1038/nature05072, September 2006.

45. Valev, D.: "Statistical relationships between the surface air temperature anomalies and the solar and geomagnetic activity indices," *Phys. Chem. Earth*, Vol. 31, pp. 109–112, doi:10.1016/j.pce.2005.03.005, January 2006.

46. de Jager, C.; and Usoskin, I.: "On possible drivers of Sun-induced climate changes," *J. Atmos. Sol.-Terr. Phys.*, Vol. 68, No. 18, pp. 2053–2060, doi:10.1016/j.jastp.2006.05.019, December 2006.

47. Kirkby, J.: "Cosmic Rays and Climate," *Sur. Geophys.*, Vol. 28, pp. 333–375, doi:10.1007/s10712-008-9030-6, March 2008.

48. Courtillot, V.; Gallet, Y.; le Mouël, J.-L.; et al.: "Are there connections between the Earth's magnetic field and climate?" *Earth Planet. Phys. Lett.*, Vol. 253, Nos. 3–4, pp. 328–339, doi: 0.1016/j.epsl.2006.10.032, January 2007.

49. Lockwood, M.; and Fröhlich, C.: "Recent oppositely directed trends in solar climate forcings and the global mean surface air temperature," *Proc. R. Soc. A*, Vol. 463, No. 2086, pp. 2447–2460, October 2007.

50. Usoskin, I.G.; and Kovaltsov, G.A.: "Cosmic rays and climate of the Earth: Possible connection," *C. R. Geoscience*, Vol. 340, No. 7, pp. 441–450, doi:10.1016/j.crte.2007.11.001, July 2008.

51. Velasco, V.M.; and Mendoza, B.: "Assessing the relationship between solar activity and some large scale climatic phenomena," *Adv. Space Res.*, Vol. 42, No. 5, pp. 866–878, doi:10.1016/j.asr.2007.05.050, September 2008.

52. de Jager, C.: "Solar activity and its influence on climate," *Neth. J. Geosci.*, Vol. 87, No. 3, pp. 207–213, 2008.

53. Wilson, R.M.: "Solar Cycle and Anthropogenic Forcing of Surface-Air Temperature at Armagh Observatory, Northern Ireland," NASA/TP—2010–216375, NASA Marshall Space Flight Center, Huntsville, AL, 28 pp., March 2010.

54. Feulner, G.; and Rahmstorf, S.: "On the effect of a new grand minimum of solar activity on the future climate on Earth," *Geophys. Res. Lett.*, Vol. 37, No. 5, 5 pp., doi:10.1029/2010GL042710, March 2010.

55. Kopp, G.; and Lean, J.L.: "A new, lower value of total solar irradiance: Evidence and climate significance," *Geophys. Res. Lett.*, Vol. 38, No. 1, 7 pp., doi:10.1029/2010GL045777, January 2011.

56. Schrijver, C.J.; Livingston, W.C.; Woods, T.N.; and Mewaldt, R.A.: "The minimal solar activity in 2008–2009 and its implications for long-term climate modeling," *Geophys. Res. Lett.*, Vol. 38, No. 6, 6 pp., doi:10.1029/2011GL046658, March 2011.

57. Wilson, R.M.: "Estimating the Mean Surface Air Temperature at Armagh Observatory, Northern Ireland, and the Global Land-Ocean Temperature Index for Sunspot Cycle 24, the Current Ongoing Sunspot Cycle," NASA/TP—2013–217484, NASA Marshall Space Flight Center, Huntsville, AL, 60 pp., July 2013.

58. Wilson, R.M.: "The Global Land-Ocean Temperature Index in Relation to Sunspot Number, the Atlantic Multidecadal Oscillation Index, the Mauna Loa Atmospheric Concentration of $CO_2$, and Anthropogenic Carbon Emissions," NASA/TP—2013–217485, NASA Marshall Space Flight Center, Huntsville, AL, 32 pp., July 2013.

59. Wilson, R.M.: "On the Trend of the Annual Mean, Maximum and Minimum Temperature and the Diurnal Temperature Range in the Armagh Observatory, Northern Ireland, Dataset, 1844–2012," NASA/TP—2013–217494, NASA Marshall Space Flight Center, Huntsville, AL, 62 pp., November 2013.

60. Gray, L.J.; Beer, J.; Geller, M.; et al.: "Solar Influences on Climate," *Rev. Geophys.*, Vol. 48, No. 4, 53 pp., doi:10.1029/2009RG000282, December 2010.

61. Herschel, W.: "Observations tending to investigate the Nature of the Sun, in order to find the Causes or Symptoms of its variable Emission of Light and Heat; with Remarks on the Use that may possibly be drawn from Solar Observations," *Philos. T. R. Soc. Lon.*, Vol. 91, pp. 265–318, doi:10.1098/rstl.1801.0015, April 1801.

62. Stauning, P.: "Solar activity–climate relations: A different approach," *J. Atmos. Sol.-Terr. Phys.*, Vol. 73, No. 13, pp. 1999–2012, doi:10.1016/j.jastp.2011.06.011, August 2011.

63. Schwabe, H.: "Sonnenuflecken," *Astron. Nachr.*, Vol. 22, No. 24, pp. 366–368, doi:10.1002/asna.18450222404, 1845.

64. Hathaway, D.H.; Wilson, R.M.; and Reichmann, E.J.: "Group Sunspot Numbers: Sunspot Cycle Characteristics," *Sol. Phys.*, Vol. 211, Nos. 1–2, pp. 357–370, doi:10.1023/A:1022425402664, December 2002.

65. Waldmeier, M.: *The Sunspot-Activity in the Years 1610-1960*, Schulthess & Co., Zürich, Germany, 171 pp., 1961.

66. Wilson, R.M.; and Hathaway, D.H.: "An Examination of Selected Geomagnetic Indices in Relation to the Sunspot Cycle," NASA/TP—2006–214711, NASA Marshall Space Flight Center, Huntsville, AL, 52 pp., December 2006.

67. Wilson, R.M.; and Hathaway, D.H.: "On the Relationship Between Solar Wind Speed, Geomagnetic Activity and the Solar Cycle Using Annual Values," NASA/TP—2008–215249, NASA Marshall Space Flight Center, Huntsville, AL, 20 pp., February 2008.

68. Wilson, R.M.; and Hathaway, D.H: "On the Relationship Between Solar Wind Speed, Earthward-Directed Coronal Mass Ejections, Geomagnetic Activity and the Sunspot Cycle Using 12-Month Moving Averages," NASA/TP—2008–215413, NASA Marshall Space Flight Center, Huntsville, AL, 90 pp., June 2008.

69. Svalgaard, L.; Cliver, E.W.; and Le Sager, P.: "IHV: a new long-term geomagnetic index," *Adv. Space Res.*, Vol. 34, No. 2, p. 436, doi:10.1016/j.asr.2003.01.029, May 2004.

70. Ohl, A.I.: "Forecast of Sunspot Maximum Number of Cycle 20," *Solice Danie*, Vol. 9, p. 84, 1966.

71. Wilson, R.M.: "On the Level of Skill in Predicting Maximum Sunspot Number: A Comparative Study of Single Variate and Bivariate Precursor Techniques," *Sol. Phys.*, Vol. 125, No. 1, p. 143, doi:10.1007/BF00154784, January 1990.

72. Hathaway, D.H.; Wilson, R.M.; and Reichmann, E.J.: "A synthesis of solar cycle prediction techniques," *J. Geophys. Res.*, Vol. 104, No. A10, p. 22,375, doi:10.1029/1999JA900313, October 1999.

73. Feynman, J.: "Geomagnetic and solar wind cycles, 1900–1975," *J. Geophys. Res.*, Vol. 87, No. A8, pp. 6153–6162, doi:10.1029/JA087iA08p06153, August 1982.

74. Feynman, J.; and Gu, X.Y.: "Prediction of geomagnetic activity on time scales of one to ten years," *Rev. Geophys.*, Vol. 24, No. 3, pp. 650–666, doi:10.1029/RG024i003p00650, August 1986.

75. Schlesinger, M.E.; and Ramankutty, N.: "An oscillation in the global climate system of period 65–70 years," *Nature*, Vol. 367, No. 6465, pp. 723–726, doi:10.1038/367723a0, February 1994.

76. Broecker, W.S.: "Thermohaline Circulation, the Achilles Heel of Our Climate System: Will Man-Made $CO_2$ Upset the Current Balance?" *Science*, Vol. 278, No. 5343, pp. 1582–1588, doi:10.1126/science.278.5343.1582, November 1997.

77. Clark, P.U.; Pisias, N.G.; Stocker, T.F.; and Weaver, A.J.: "The role of the thermohaline circulation in abrupt climate change," *Nature*, Vol. 415, No. 6874, pp. 863–869, doi:10.1038/415863a, February 2002.

78. Dijkstra, H.A.; te Raa, L.; Schmeits, M.; and Gerrits, J.: "On the physics of the Atlantic Multidecadal Oscillation," *Ocean Dynam.*, Vol. 56, No. 1, pp. 36–50, doi:10.1007/s10236-005-0043-0, May 2006.

79. Grossmann, I.; and Klotzbach, P.J.: "A review of North Atlantic modes of natural variability and their driving mechanisms," *J. Geophys. Res.*, Vol. 114, No. D24, 14 pp., doi:10.1029/2009JD012728, December 2009.

80. Ropelewski, C.F.; and Halpert, M.S.: "Precipitation Patterns Associated with the High Index Phase of the Southern Oscillation," *J. Climate*, Vol. 2, No. 3, pp. 594–614, doi:10.1175/1520-0442(1989)002<0268:PPAWTH>2.0.CO;2, March 1989.

81. Glantz, M.H.; Katz, R.W.; and Nicholls, N. (eds.): *Teleconnections Linking Worldwide Climate Anomalies*, Cambridge University Press, Cambridge, NY, 535 pp., 1991.

82. Hurrell, J.W.; Kushnir, Y.; and Visbeck, M.: "The North Atlantic Oscillation," *Science*, Vol. 291, No. 5504, pp. 603–605, doi:10.1126/science.1058761, January 2001.

83. Visbeck, M.H.; Hurrell, J.W.; Polvani, L.; and Cullen, H.M.: "The North Atlantic Oscillation: Past, present, and future," *Proc. Natl. Acad. Sci. USA*, Vol. 98, No. 23, pp. 12,876–12,877, doi:10.1073/pnas.231391598, November 2001.

84. Hurrell, J.W.; Kushnir, Y.; Ottersen, G.; and Visbeck, M. (eds.): *The North Atlantic Oscillation*: *Climatic Significance and Environmental Impact*, in *Geophys. Monogr. Ser.*, Vol. 134, American Geophysical Union, Washington, DC, 279 pp., doi:10.1029/GM134, 2003.

85. Hurrell, J.W.; and Deser, C.: "North Atlantic climate variability: The role of the North Atlantic Oscillation," *J. Marine Syst.*, Vol. 79, Nos. 3–4, pp. 231–244, doi:10.1016/j.jmarsys.2008.11.026, February 2010.

86. Minobe, S.: "A 50–70 year climatic oscillation over the North Pacific and North America," *Geophys. Res. Lett.*, Vol. 24, No. 6, pp. 683–686, doi:10.1029/97GL00504, March 1997.

87. Gershunov, A.; and Barnett, T.P.: "Interdecadal Modulation of ENSO Teleconnections," *Bull. Am. Meteor. Soc.*, Vol. 79, No. 12, pp. 2715–2725, doi:10.1175/1520-0477(1998)079<2715:IMOET>2.0.CO;2, December 1998.

88. Mantua, N.J.; and Hare, S.R.: "The Pacific Decadal Oscillation," *J. Oceanogr.*, Vol. 58, No. 1, pp. 35–44, doi:10.1023/A:1015820616384, February 2002.

89. Keeling, C.D.: "The Concentration and Isotropic Abundances of Carbon Dioxide in the Atmosphere," *Tellus*, Vol. 12, No. 2, pp. 200–203, doi:10.1111/j.2153-3490.1960.tb01300.x, May 1960.

90. Bolin, B.; and Keeling, C.D.: "Large-scale atmospheric mixing as deduced from seasonal and meridional variations of carbon dioxide," *J. Geophys. Res.*, Vol. 68, No. 13, pp. 3899–3920, doi:10.1029/JZ068i013p03899, July 1963.

91. Pales, J.C.; and Keeling, C.D.: "The concentration of atmospheric carbon dioxide in Hawaii," *J. Geophys. Res.*, Vol. 70, No. 24, pp. 6053–6076, doi:10.1029/JZ070i024p06053, December 1965.

92. Brown, C.W.; and Keeling, C.D.: "The concentration of atmospheric carbon dioxide in Antarctica," *J. Geophys. Res.*, Vol. 70, No. 24, pp. 6077–6085, doi:10.1029/JZ070i024p06077, December 1965.

93. Bolin, B.; and Bischof, W.: "Variations of the carbon dioxide content of the atmosphere in the northern hemisphere," *Tellus*, Vol. 22, No. 4, pp. 431–442, doi:10.1111/j.2153-3490.1970.tb00508.x, August 1970.

94. Bacastow, R.B.; Keeling, C.D.; and Whorf, T.P.: "Seasonal amplitude increase in atmospheric $CO_2$ concentration at Mauna Loa, Hawaii, 1959–1982," *J. Geophys. Res.*, Vol. 90, No. D6, pp. 10,529–10,540, doi:10.1029/JD090iD06p10529, October 1985.

95. Thoning, K.W.; Tans, P.P.; and Komhyr, W.D.: "Atmospheric carbon dioxide at Mauna Loa Observatory: 2. Analysis of the NOAA GMCC data, 1974–1985," *J. Geophys. Res.*, Vol. 94, No. D6, pp. 8549–8565, doi:10.1029/JD094iD06p08549, June 1989.

96. Solheim, J.-E.; Stordahl, K.; and Humlum, O.: "Solar Activity and Svalbard Temperatures," *Adv. Meteor.*, Vol. 2011, No. 534146, 8 pp., doi:10.1155/2011/543146, November 2011.

97. Solheim, J.-E.; Stordahl, K.; and Humlum, O.: "The long sunspot cycle 23 predicts a significant temperature decrease in cycle 24," *J. Atmos. Sol.-Terr. Phys.*, Vol. 80, pp. 267–284, doi:10.1016/j.jastp.2012.02.008, May 2012.

98. Willson, R.C.: "Solar irradiance variations and solar activity," *J. Geophys. Res.*, Vol. 87, No. A6, pp. 4319–4326, doi:10.1029/JA087iA06p04319, June 1982.

99. Willson, R.C.; and Hudson, H.S.: "Solar luminosity variations in solar cycle 21," *Nature*, Vol. 332, No. 6167, pp. 810–812, doi:10.1038/332810a0, April 1988.

100. Chapman, G.A.; Cookson, A.M.; and Dobias, J.J.: "Variations in total solar irradiance during solar cycle 22," *J. Geophys. Res.*, Vol. 101, No. A6, pp. 13,541–13,548, doi:10.1029/96JA00683, June 1996.

101. Pap, J.M.; and Fröhlich, C.: "Total Solar Irradiance Variations," *J. Atmos. Sol.-Terr. Phys.*, Vol. 61, Nos. 1–2, pp. 15–24, doi:10.1016/S1364-6826(98)00112-6, January 1999.

102. Solanki, S.K.; and Fligge, M.: "Solar irradiance variations and climate," *J. Atmos. Sol.-Terr. Phys.*, Vol. 64, Nos. 5–6, pp. 677–685, doi:10.1016/S1364-6826(02)00029-9, March–April 2002.

103. Pap, J.M.; Turmon, M.; Floyd, L.; et al.: "Total solar and spectral irradiance variations from solar cycles 21 to 23," *Adv. Space Res.*, Vol. 29, No. 12, pp. 1923–1932, doi:10.1016/S0273-1177(02)00237-5, June 2002.

104. Lohmann, G.; Rimbu, N.; and Dima, M.: "Climate signature of solar irradiance variations: analysis of long-term instrumental, historical, and proxy data," *Intern. J. Climatol.*, Vol. 24, No. 8, pp. 1045–1056, doi:10.1002/joc.1054, June 2004.

105. Foukal, P.; Fröhlich, C.; Spruit, H.; and Wigley, T.M.L.: "Variations in solar luminosity and their effect on the Earth's climate," *Nature*, Vol. 443, pp. 161–166, doi:10.1038/nature05072, September 2006.

106. Kelly, P.M.; and Wigley, T.M.L.: "Solar cycle length, greenhouse forcing and global climate," *Nature*, Vol. 360, pp. 328–330, doi:10.1038/360328a0, November 1992.

107. Schlesinger, M.E.; and Ramankutty, N.: "Implications for global warming of intercycle solar irradiance variations," *Nature*, Vol. 360, No. 6402, pp. 330–333, doi:10.1038/360330a0, November 1992.

108. Andronova, N.G.; and Schlesinger, M.E.: "Causes of global temperature changes during the 19th and 20th centuries," *Geophys. Res. Lett.*, Vol. 27, No. 14, pp. 2137–2140, doi:10.1029/2000GL006109, July 2000.

109. Sherwood, S.C.; Bony, S.; and Dufresne, J.-L.: "Spread in model climate sensitivity traced to atmospheric convective mixing," *Nature*, Vol. 505, No. 7481, pp. 37–42, doi:10.1038/nature12829, January 2014.

# REPORT DOCUMENTATION PAGE

*Form Approved*
*OMB No. 0704-0188*



| 1. REPORT DATE *(DD-MM-YYYY)* | 2. REPORT TYPE | 3. DATES COVERED *(From - To)* |
|---|---|---|
| 01–04–2014 | Technical Publication | |

**4. TITLE AND SUBTITLE**

On the Relationship Between Global Land-Ocean Temperature and Various Descriptors of Solar-Geomagnetic Activity and Climate

**5a. CONTRACT NUMBER**

**5b. GRANT NUMBER**

**5c. PROGRAM ELEMENT NUMBER**

**6. AUTHOR(S)**

Robert M. Wilson

**5d. PROJECT NUMBER**

**5e. TASK NUMBER**

**5f. WORK UNIT NUMBER**

**7. PERFORMING ORGANIZATION NAME(S) AND ADDRESS(ES)**

George C. Marshall Space Flight Center
Huntsville, AL 35812

**8. PERFORMING ORGANIZATION REPORT NUMBER**

M–1382

**9. SPONSORING/MONITORING AGENCY NAME(S) AND ADDRESS(ES)**

National Aeronautics and Space Administration
Washington, DC 20546–0001

**10. SPONSORING/MONITOR'S ACRONYM(S)**

NASA

**11. SPONSORING/MONITORING REPORT NUMBER**

NASA/TP—2014–218193

**12. DISTRIBUTION/AVAILABILITY STATEMENT**

Unclassified-Unlimited
Subject Category 47
Availability: NASA STI Information Desk (757–864–9658)

**13. SUPPLEMENTARY NOTES**

Prepared by the Science and Research Office, Science and Technology Office

**14. ABSTRACT**

Examined are sunspot cycle- (SC-) length averages of the annual January–December values of the Global Land-Ocean Temperature Index (<GLOTI>) in relation to SC-length averages of annual values of various descriptors of solar-geomagnetic activity and climate, incorporating lags of 0–5 yr. For the overall interval SC12–SC23, the <GLOTI> is inferred to correlate best against the parameter <aa(I:SSN)> incorporating lag = 5 yr, where the parameter <aa(I:SSN)> refers to the resultant aa value having removed that portion of the annual aa average value due to the yearly variation of sunspot number (SSN). The inferred correlation between the <GLOTI> and <aa(I:SSN)> is statistically important at confidence level $cl > 99.9\%$, having a coefficient of linear correlation $r = 0.865$ and standard error of estimate $se = 0.149$ °C. Excluding the most recent cycles SC22 and SC23, the inferred correlation is stronger, having $r = 0.969$ and $se = 0.048$ °C. With respect to the overall trend in the <GLOTI>, which has been upwards towards warmer temperatures since SC12 (1878–1888), solar-geomagnetic activity parameters are now trending downwards (since SC19). For SC20–SC23, in contrast, comparison of the <GLOTI> against SC-length averages of the annual value of the Mauna Loa carbon dioxide (<MLCO2>) index is found to be highly statistically important ($cl » 99.9\%$), having $r = 0.9994$ and $se = 0.012$ °C for lag = 2 yr. On the basis of the inferred preferential linear correlation between the <GLOTI> and <MLCO2>, the current ongoing SC24 is inferred to have <GLOTI> warmer than was seen in SC23 (i.e., >0.526 °C), probably in excess of 0.68 °C (relative to the 1951–1980 base period).

**15. SUBJECT TERMS**

Global Land-Ocean Temperature Index, climatic change, climate, sunspot cycle

| 16. SECURITY CLASSIFICATION OF: | | | 17. LIMITATION OF ABSTRACT | 18. NUMBER OF PAGES | 19a. NAME OF RESPONSIBLE PERSON |
|---|---|---|---|---|---|
| a. REPORT | b. ABSTRACT | c. THIS PAGE | | | STI Help Desk at email: help@sti.nasa.gov |
| U | U | U | UU | 62 | 19b. TELEPHONE NUMBER *(Include area code)* STI Help Desk at: 757–864–9658 |

National Aeronautics and
Space Administration
IS20
**George C. Marshall Space Flight Center**
Huntsville, Alabama 35812